

Serveur Académique Lausannois SERVAL [serval.unil.ch](http://serval.unil.ch)

## Author Manuscript

Faculty of Biology and Medicine Publication

This paper has been peer-reviewed but does not include the final publisher proof-corrections or journal pagination.

Published in final edited form as:

**Title:** Early expression of the type III secretion system of *Parachlamydia acanthamoebae* during a replicative cycle within its natural host cell *Acanthamoeba castellanii*.

**Authors:** Croxatto A, Murset V, Chassot B, Greub G

**Journal:** Pathogens and disease

**Year:** 2013 Dec

**Volume:** 69

**Issue:** 3

**Pages:** 159-75

**DOI:** 10.1111/2049-632X.12065

In the absence of a copyright statement, users should assume that standard copyright protection applies, unless the article contains an explicit statement to the contrary. In case of doubt, contact the journal publisher to verify the copyright status of an article.

1  
2  
3 **Early expression of the Type III secretion system of *Parachlamydia acanthamoebae***  
4  
5 **during a replicative cycle within its natural host cell *Acanthamoeba castellanii*.**  
6

7 Antony Croxatto, Valérie Murset<sup>§</sup>, Bérénice Chassot<sup>#</sup> and Gilbert Greub\*  
8  
9

10  
11  
12 Center for Research on Intracellular Bacteria (CRIB), Institute of Microbiology, University Hospital  
13  
14 Center and University of Lausanne, Lausanne, Switzerland  
15  
16

17  
18  
19  
20 Running title: Type III secretion of *Parachlamydia acanthamoebae*.  
21  
22

23  
24  
25  
26 Contents category: Cell and Molecular Biology of Microbes  
27  
28

29  
30  
31 \*Correspondence and reprints  
32

33 Gilbert Greub, MD PhD  
34

35 Center for Research on Intracellular Bacteria  
36

37 Institute of Microbiology  
38

39 University Hospital Center and University of Lausanne  
40

41 1011 Lausanne  
42

43 SWITZERLAND  
44

45 Phone: (00) 41 21 314 49 79  
46

47 Fax: (00) 41 21 314 40 60  
48

49 Email: [gilbert.greub@chuv.ch](mailto:gilbert.greub@chuv.ch)  
50  
51

52  
53 <sup>§</sup>Present address: Institute of Microbiology, ETH Zürich, Switzerland.  
54

55 <sup>#</sup>Present address: Zoology, Department of Biology, University of Fribourg, Switzerland.  
56  
57  
58  
59  
60

## Summary

The type three secretion system (T3SS) operons of *Chlamydiales* bacteria are distributed in different clusters along their chromosomes and are conserved both at the level of sequence and genetic organization. A complete characterization of the temporal expression of multiple T3SS components at the transcriptional and protein levels has been performed in *Parachlamydia acanthamoebae* replicating in its natural host cell *Acanthamoeba castellanii*. The T3SS components were classified in 4 different temporal clusters depending on their pattern of expression during the early, mid and late-phases of the infectious cycle. The putative T3SS transcription units predicted in *Parachlamydia* are similar to those described in *C. trachomatis*, suggesting that T3SS units of transcriptional expression are highly conserved among *Chlamydiales* bacteria. The maximal expression and activation of the T3SS of *Parachlamydia* occurred during the early to mid-phase of the infectious cycle corresponding to a critical phase during which the intracellular bacterium has (i) to evade and/or block the lytic pathway of the amoeba, (ii) to differentiate from elementary bodies (EBs) to reticulate bodies (RBs) and (iii) to modulate the maturation of its vacuole to create a replicative niche able to sustain efficient bacterial growth.

## 1 Introduction

2 The *Chlamydiales* order currently includes the *Chlamydiaceae*, *Parachlamydiaceae*, *Waddliaceae*,  
3 *Simkaniaceae*, *Criblamydiaceae* and *Rhabdochlamydiaceae* families (Corsaro and Greub, 2006).

4 *Parachlamydiaceae* naturally resist destruction by free-living amoebae. These obligate intracellular  
5 bacteria may use the protistan host as a training ground to select virulence traits that help them to resist  
6 to the microbicidal effectors of amoebae and macrophages (Greub, 2009; Greub and Raoult, 2004).

7 *Parachlamydia acanthamoebae* is a bacterium belonging to the *Parachlamydiaceae* family. *P.*  
8 *acanthamoebae* is seriously suspected to be involved in respiratory tract infections (Greub, 2009;  
9 Lamoth and Greub, 2009) since serological and molecular evidences are supporting its role as a human  
10 respiratory pathogen, mainly in patients with community-acquired (Greub *et al.*, 2003b) and aspiration  
11 pneumonia (Greub *et al.*, 2003c). In addition, the disease has been reproduced in a murine model  
12 following both intranasal and intratracheal bacterial inoculation (Casson *et al.*, 2008).

13 The pathogenic potential of *Parachlamydia* is further supported by the ability of this obligate  
14 intracellular bacteria to enter and replicate in human macrophages (Greub *et al.*, 2003a), by preventing  
15 the secretion of proinflammatory cytokines (Greub *et al.*, 2005a) and the fusion of its endocytic  
16 vacuole with the lysosome (Greub *et al.*, 2005b). Moreover, *Parachlamydia* is also able to enter and  
17 replicate in pneumocytes and lung fibroblasts (Casson *et al.*, 2006).

18 Members of the *Chlamydiales* are characterized by a biphasic development cycle comprising the  
19 infectious elementary bodies (EBs) and the replicating reticulate bodies (EBs). They have evolved  
20 from a common ancestor since more than 700 million years (Greub and Raoult, 2003) that has  
21 developed mechanisms for intracellular survival and multiplication in primitive unicellular eukaryotes.

22 Consequently, *Chlamydia*-related bacteria and classical *Chlamydia* share a “core genome” of about  
23 700 ORFs that encode for essential bacterial functions that guarantee an efficient intracellular lifestyle  
24 including several virulence mechanisms such as the Type III secretion system (T3SS) (Collingro *et al.*,  
25 2011b; Bertelli *et al.*, 2010; Greub *et al.*, 2009; Horn *et al.*, 2004).

1  
2  
3 26 T3SS mediates the translocation of bacterial effectors to the cytosol of infected cells to modulate  
4  
5 27 various host cell functions facilitating the survival and the replication of the bacterial pathogens  
6  
7 28 (Coburn *et al.*, 2007). The proteins that constitute the T3SS secretory apparatus are termed structural  
8  
9 29 proteins. An additional set of proteins termed “translocators” function by translocating virulence  
10  
11 30 factors called “effector” proteins into the host cell cytoplasm. T3SS genes are present in all *Chlamydia*  
12  
13 31 species examined to date and suggest that T3SS is essential for the survival of these strict intracellular  
14  
15 32 bacteria. Proteins that compose the T3SS secretory apparatus and translocators are for the most part  
16  
17 33 well conserved structurally and functionally among *Chlamydiales* spp. and genes encoding for these  
18  
19 34 T3SS proteins are found in distinct conserved genomic clusters (Betts *et al.*, 2008a; Peters *et al.*,  
20  
21 35 2007). In contrast, T3SS effectors display little sequence homology and are much harder to identify,  
22  
23 36 except for some members of the family of T3SS secreted Inc proteins which are characterized by a  
24  
25 37 large bi-lobed hydrophobic domain that serves to anchor the proteins in the inclusion membrane  
26  
27 38 (Bannantine *et al.*, 2000). Effectors being the direct modulators of host cell functions and of unique  
28  
29 39 pathogenic properties, every bacterium has adapted its pool of effectors to survive and replicate in  
30  
31 40 their respective environmental niches, which likely explained the poor sequence conservation among  
32  
33 41 these secreted proteins. However, effectors proteins often display common structural traits and have  
34  
35 42 similar enzymatic activities among various bacterial species, including cytoskeletal rearrangement,  
36  
37 43 subversion of signaling pathways, activation or inhibition of apoptosis and modulation of intracellular  
38  
39 44 trafficking (Mota and Cornelis, 2005). In *Chlamydiales*, effector proteins are secreted in the inclusion  
40  
41 45 lumen, inserted in the inclusion membrane or translocated in the cytosol of the host cell. A few  
42  
43 46 effectors have been identified so far in *Chlamydiaceae* including Tarp, inclusion membrane proteins  
44  
45 47 IncA to IncG, CADD, Mip and CopN (Beeckman and Vanrompay, 2010; Subtil *et al.*, 2005;  
46  
47 48 Bannantine *et al.*, 2000).

49  
50 49 The secretory apparatus is composed of about 20 proteins. The functions of the proteins that compose  
51  
52 50 the injectisome of *Chlamydiales* bacteria have been mainly attributed based on sequence similarities  
53  
54 51 with proteins composing well described heterologous T3SS apparatus of other bacteria species such as  
55  
56 52 *Yersinia* and *Salmonella* (Hueck, 1998). Several studies indicate that the secretin-like SctC protein  
57  
58  
59  
60

1  
2  
3 53 form the outer membrane (OM) ring which is connected to the inner membrane (IM) ring through  
4  
5 54 SctD. The inner membrane (IM) ring is formed by SctD together with the lipoprotein SctJ. In the  
6  
7 55 *Yersinia* T3SS apparatus, the IM ring is associated with a multi-components complex composed of (i)  
8  
9 56 Sct R/S/T/U/V (proteins associated with the export apparatus), of (ii) Sct N/L (ATPase associated  
10  
11 57 proteins) and of (iii) SctQ which form the cytosolic ring (C-ring) (Diepold *et al.*, 2010; Cornelis,  
12  
13 58 2002). Several studies focusing on T3SS protein interactions in *Chlamydia* indicate that the  
14  
15 59 *Chlamydiales* T3SS apparatus is very similar in structure and function compared to the well studied  
16  
17 60 apparatus of *Yersinia* and other species (Betts-Hampikian and Fields, 2010; Fields, 2006).

18  
19  
20 61 Recent experimental evidences obtained in the *Yersinia* model suggest that the apparatus assembly is  
21  
22 62 initiated by the formation of the SctC OM ring and proceed inwards through the assembly of the IM  
23  
24 63 ring SctD and SctJ. Upon completion of the IM ring, additional T3SS components are recruited to the  
25  
26 64 basal apparatus to complete the export apparatus and to form the ATPase and C-ring complexes.  
27  
28 65 Finally, the needle consisted by SctF is assembled to form a mature and functional T3SS. Unlike  
29  
30 66 SctN/L/Q, the exact temporal integration of the IM proteins SctR/S/T/U/V remained unclear (Diepold  
31  
32 67 *et al.*, 2010).

33  
34  
35 68 Considering the central role of T3SS in *Chlamydiales* biology, a thorough characterization of T3SS  
36  
37 69 expression of conserved components throughout an infectious cycle of *Parachlamydia* within  
38  
39 70 *Acanthamoeba castellanii* amoeba was conducted. We showed that T3SS conservation among  
40  
41 71 *Chlamydiales* is not only restricted to genomic sequence and organization but is also observed at the  
42  
43 72 level of temporal expression during the development cycle.

## 44 45 46 73 Results

### 47 48 49 74 **Temporal characterization of an infectious cycle**

50  
51  
52 75 A thorough characterization of the different stages that compose a complete infectious cycle of  
53  
54 76 *Parachlamydia* within *A. castellanii* was required to accurately define temporal key stages of the  
55  
56 77 internalization, differentiation, replication and extrusion of *Parachlamydia* during a replicative cycle.

1  
2  
3 78 Amoebae were infected with a MOI of 10 to ensure a nearly 100% rate of infection allowing thus the  
4  
5 79 study of a single replication cycle. As shown by confocal microscopy, between 5 to 10 infectious  
6  
7 80 bacteria were internalized into amoebae 1h post-infection (Figure 1A). The differentiation of EBs into  
8  
9 81 RBs was mostly completed 5h post-infection and inclusions containing multiple replicating bacteria  
10  
11 82 were observed 8h post-infection. Following a lag-phase characterized by the differentiation of EBs  
12  
13 83 into RBs, an exponential growth is observed between 5 and 16h post-infection as shown by  
14  
15 84 quantitative PCR (Figure 1B). The bacterial growth enters stationary-phase between 16h and 24h post-  
16  
17 85 infection which corresponds to the beginning of the re-differentiation of RBs into EBs (Figure 1A and  
18  
19 86 B). As shown in figure 1A, most of the amoebae are lysed 48h post-infection, releasing EBs in the  
20  
21 87 extracellular environment. Based on these data, the infectious cycle was classified as early-, mid-, and  
22  
23 88 late cycles. These times correspond to key developmental stages with (1) early cycle during which  
24  
25 89 bacteria are internalized in the host cell and differentiate from EBs into RBs, (2) mid cycle  
26  
27 90 characterized by exponential growth of dividing RBs and (3), late cycle consisting of the end of  
28  
29 91 bacterial growth, re-differentiation of RBs into EBs and finally release of EBs into the extracellular  
30  
31 92 environment (Figure 1C).

### 33 34 93 **Identification of 16S rRNA as an optimal internal control to measure relative transcriptional** 35 36 94 **expression during a replicative cycle**

37  
38  
39 95 *Chlamydiales* EBs and RBs are two developmental forms characterized by profound differences in  
40  
41 96 membrane composition and structure that play an important role in the efficiency of bacterial lysis  
42  
43 97 during DNA and RNA extraction procedures. Several lysis protocols compatible with the Promega  
44  
45 98 Wizard SV Genomic DNA Purification kit have been evaluated on samples collected at different times  
46  
47 99 corresponding to the different developmental stages that characterize the growth of *Parachlamydia*  
48  
49 100 within *A. castellanii*. These experiments showed that a specific lysis protocol including an incubation  
50  
51 101 of 2 hours with proteinase K at 55°C has to be followed to ensure efficient lysis of both EBs and RBs  
52  
53 102 since an incomplete lysis of EBs was obtained in absence of proteinase K treatment as measured by  
54  
55 103 quantitative real time PCR of the 16S rDNA gene (figure 2 and supplementary figure 1). Thus, a  
56  
57 104 reduced amount of 16S rDNA was observed in absence of proteinase K treatment for samples  
58  
59  
60

1  
2  
3 105 collected during early (0 to 4h post infection) and late-phase (36 to 48h post infection) of the  
4  
5 106 replicative cycle that are characterized by a significant presence of EBs whereas no difference was  
6  
7 107 measured during the mid-phase (8h to 24h) which is characterized by the sole presence of replicating  
8  
9 108 RBs.

10  
11 109 The extraction of integral bacterial RNA is incompatible with proteinase K treatment at 55°C for 2  
12  
13 110 hours. Thus, the transcriptional expression measured by quantitative reverse transcription PCR (qRT-  
14  
15 111 PCR) of several putative constitutively expressed housekeeping genes including *16S rRNA*, *gyrB*,  
16  
17 112 *secY*, *rpoB* and *hsp60* was compared to the amount of 16S rDNA extracted without proteinase K and  
18  
19 113 measured by qPCR during a replicative cycle of *Parachlamydia* in *A. castellanii* (Figure 2). The fold  
20  
21 114 increase of the different RNAs compared to the 16S rDNA showed that only the *16S rRNA* was  
22  
23 115 constitutively expressed during a replicative cycle (Figure 2A). The ratio of 16S rRNA / 16S rDNA  
24  
25 116 was of about 1 at each time measured during a replicative cycle whereas the ratio observed between  
26  
27 117 other transcripts with the 16S rDNA was greatly varying during the infectious cycle (Figure 2B).  
28  
29 118 Thus, the normalized expression of *gyrB*, *secY*, *rpoB* and *hsp60* relatively to *16S rRNA* demonstrated  
30  
31 119 that the expression of these essential housekeeping genes is rapidly induced following bacterial  
32  
33 120 internalization (Figure 2C). The transcriptional expression of these genes is then decreasing during the  
34  
35 121 late mid-phase of the replicative cycle when bacteria begin to convert from RBs to EBs. As a control,  
36  
37 122 the transcriptional expression of *hc-1*, the homolog of *Chlamydia trachomatis* *hctB* expressed during  
38  
39 123 RB to EB conversion, was measured during a replicative cycle (Figure 2). Similar to *hctB*, *hc-1*  
40  
41 124 exhibited an increased expression in the late mid-phase corresponding to the beginning of re-  
42  
43 125 differentiation of RBs into EBs. Together, these data indicate that the amount of measured *16S rRNA*  
44  
45 126 transcripts reflects bacterial growth and can be thus considered as an optimal internal control to  
46  
47 127 measure relative transcriptional expression of the T3SS genes of *Parachlamydia* during a replicative  
48  
49 128 cycle within *A. castellanii*.

50  
51  
52  
53 129

54  
55  
56 130  
57  
58  
59  
60

1  
2  
3 131 **Temporal transcriptional expression of T3SS components.**  
4

5  
6 132 Similar to other *Chlamydiae*, genes encoding for T3SS apparatus components are located in distinct  
7  
8 133 genomic clusters distributed along the chromosome (Figure 3A). Four genomic clusters containing  
9  
10 134 conserved genes encoding for the injectisome and the translocon apparatus and exhibiting a very  
11  
12 135 similar genetic organization than other *Chlamydiae* were identified in the genome of *Parachlamydia*  
13  
14 136 (Greub *et al.*, 2009). Unlike *Chlamydiaceae*, no gene showing homology with the flagellar system and  
15  
16 137 having a possible function in chlamydial T3SSs have been identified in the genome of *Parachlamydia*.  
17  
18 138 Thus, the transcriptional expression of the mRNA transcripts of every gene encoding for a protein with  
19  
20 139 a known function was analyzed by qRT-PCR (Figure 3B). The expression of the various T3SS genes  
21  
22 140 during the developmental cycle could be classified in 4 temporal expression clusters (Figure 3B). The  
23  
24 141 first cluster composed of the *copB*, *syncDI* and *sctU* is characterized by a marked repression or lack of  
25  
26 142 activation during the early and mid-phases followed by a significant increased expression in the late-  
27  
28 143 phase (Figure 3B, EL). The second cluster including the *sct Q/W/F/E/G/V/N* genes is characterized by  
29  
30 144 a basal expression during the early and mid-phases and a significant increased expression during the  
31  
32 145 late-phase (Figure 3B, L). The third cluster composed of *sctC/L/J/T* and the multi-cargo secretion  
33  
34 146 chaperone *mcsc* includes genes that exhibit a dramatic increased expression in the early and mid-  
35  
36 147 phases followed by a decreased basal expression during the late-phase (Figure 3B, E). Finally, the  
37  
38 148 fourth temporal cluster is composed of the putative predicted T3SS secreted effector *pkn5* and of a  
39  
40 149 *Parachlamydia* secreted protein localizing to the replicative inclusion membrane (PahN) that are both  
41  
42 150 significantly highly expressed during the mid and beginning of late-phase (Figure 3B, M).  
43  
44

45 151 Following normalization of expression with the highest temporal expression assigned to 100 and the  
46  
47 152 lowest to 0, a temporal matrix composed of the transcriptional expression of the measured T3SS genes  
48  
49 153 was generated (Figure 4A). These analyses strongly suggest that the expression of the genes that  
50  
51 154 encode for T3SS components can be classified in 4 major defined temporal clusters of gene expression  
52  
53 155 composed of early (E), early-late (EL), mid (M) and late (L) phase-expressed genes.  
54  
55  
56  
57  
58  
59  
60

1  
2  
3 156 A bioinformatic analysis of the T3SS genomic clusters loci was performed with the fgenesB software  
4  
5 157 to predict transcriptional units and compared with mRNA expression analysis of T3SS genes. Except  
6  
7 158 for one gene (*pkn5*), the experimental qRT-PCR gene expression data are congruent with the *in silico*  
8  
9 159 prediction (Figure 4B) showing no discrepancies between temporal gene expression and association to  
10  
11 160 a predicted transcriptional unit. Thus *sctU* and *sycD1/copB* (cluster EL), *sctC* and *sctJ/L/T* (cluster E),  
12  
13 161 *sctE/F/G/N/Q* (cluster L), *sctV/sycE* (cluster L) are all located in distinct transcriptional units  
14  
15 162 corresponding to defined temporal clusters (Figure 4). Moreover, the *C. trachomatis* T3SS genes  
16  
17 163 transcriptional expression study performed by Hefty *et al.* (Hefty and Stephens, 2007) strongly  
18  
19 164 indicates that transcriptional expression units of T3SS genes are highly similar between  
20  
21 165 *Parachlamydia* and *C. trachomatis* (Figure 4B). Together these data suggest that T3SSs in  
22  
23 166 *Chlamydiales* are not only conserved at the level of genetic sequence and organization, but also at the  
24  
25 167 level of gene expression.

#### 26 27 28 168 **Temporal protein expression measurement by western blotting: limitations of the technique.**

29  
30  
31 169 Even though transcription and translation in bacteria are very often coupled, an analysis of protein  
32  
33 170 expression throughout an infectious cycle has to be performed to confirm that a similar temporal  
34  
35 171 expression of T3SS genes and their respective encoded proteins is observed. Proteins encoded by  
36  
37 172 genes belonging to different temporal clusters were selected for protein purifications and mouse  
38  
39 173 immunization programs. Two proteins, Mcsc and SctJ, encoded by genes expressed during early and  
40  
41 174 mid-phase (temporal cluster E), two proteins, CopB and SycD (Scc2), encoded by genes expressed  
42  
43 175 during the early and late-phase (temporal cluster EL) , and CopN (SctW) encoded by a gene expressed  
44  
45 176 during the late-phase (temporal cluster L) were selected. The antisera specificity and the protein  
46  
47 177 expression at different times of the infectious cycle were measure by western blot using specific  
48  
49 178 antibodies (Figure 5). A major drawback of measuring comparative protein amounts during the  
50  
51 179 bacterial growth of obligate intracellular bacteria is the difficulty to normalize the amount of total  
52  
53 180 bacterial proteins collected at different times during the replication cycle. An increased in specific  
54  
55 181 proteins amounts in the late-phase of the replicative cycle may only be due to a significant increased in  
56  
57 182 bacterial numbers and not to a specific up-regulation of protein expression. Thus, specific antiserum

1  
2  
3 183 raised against whole bacterial cells was used as an internal control to monitor bacterial growth during  
4  
5 184 the development cycle. The expression of SycD and Mesc was poorly or not detected by western blot  
6  
7 185 before the late-phase of the replicative cycle hindering the possibility to measure their relative  
8  
9 186 expression throughout parachlamydial growth within *A. castellanii*. An estimation of the relative  
10  
11 187 expression of CopB, CopN (SctW) and SctJ during the infectious cycle was calculated by normalizing  
12  
13 188 the measured intensity of the band corresponding to the various proteins to the intensity of the signal  
14  
15 189 corresponding to the whole bacterial cells (Supplementary figure 2). Similar to gene expression  
16  
17 190 analysis of *copB* and *copN* (*SctW*), an increasing amount of the protein CopB and CopN (SctW) was  
18  
19 191 observed in the late-phase of the bacterial replicative cycle. Interestingly, a high relative amount of  
20  
21 192 these proteins was also observed at 8hr suggesting that late-phase synthesized proteins of the T3SS are  
22  
23 193 likely functional and still present in high amount during the early-phase of subsequent infection  
24  
25 194 cycles. The protein encoded by the early transcribed gene *sctJ* exhibited the highest relative expression  
26  
27 195 at 8h confirming that de novo SctJ protein synthesis is likely occurring during the early-phase of the  
28  
29 196 infection (Supplementary figure 2). Unfortunately, the amount of bacteria present during the very  
30  
31 197 early-phase of infection is very low and the expression of the analyzed proteins was not detected  
32  
33 198 before 8h post-infection hindering the possibility to accurately monitor protein expression by western  
34  
35 199 blot during the critical first hours of the infectious cycle. In addition, the relative intensity measured at  
36  
37 200 early time of infection by western blot is subjected to imprecision due to very low signal detection.  
38  
39 201 Thus, an alternative method to obtain more accurate protein expression measurement during the entire  
40  
41 202 replicative cycle is required.

### 44 203 **Temporal protein expression measurement by quantitative immunofluorescence.**

46  
47 204 To circumvent western blotting experimental limitations, a quantitative immunofluorescence method  
48  
49 205 proposed by Noursadeghi et al. (Noursadeghi *et al.*, 2008) was adapted to measure bacterial single cell  
50  
51 206 protein expression by quantitative immunofluorescence confocal microscopy (Figure 6). This method  
52  
53 207 relies on the measurement of the summing of protein signals from multiple focus plans covering the  
54  
55 208 entire thickness of the sample. Quantitative fluorescence data are then obtained by generating the  
56  
57 209 histogram of the signal intensity of a Z-projection obtained by summing multiple focal slices. Using

1  
2  
3 210 this methodology, the protein expression of the late-cycle expressed gene *copB* was analysed during a  
4  
5 211 complete replicative cycle by using a specific anti-CopB mouse anti-sera (Figure 7). Quantitative  
6  
7 212 immunofluorescence histograms were generated for several time points post-infection and showed that  
8  
9 213 the protein CopB is expressed during late-cycle phase, confirming a late-cycle expression of the T3SS  
10  
11 214 component CopB. The same analysis was applied to the Mscs, SctJ, PahN and SctW (CopN) proteins  
12  
13 215 (Figure 8). Similar to CopB, the temporal expression of these 4 proteins were congruent with the  
14  
15 216 temporal expression of their respective mRNA transcripts (Figure 8 and 3B). The chaperone Mscs and  
16  
17 217 the inner membrane components SctJ were expressed in higher amount 2h and 8h post-infection,  
18  
19 218 during the early and mid-phase cycles, followed by a marked reduced signal intensity observed from  
20  
21 219 16h post-infection which corresponds to the entry into late-cycle phase. The histogram intensity of the  
22  
23 220 late transcribed gene encoded protein SctW (CopN) showed a gradual reduction of the protein amount  
24  
25 221 from 2h to 16h, indicating that a relative high amount of proteins are present in EBs and in early  
26  
27 222 differentiated RBs during the first phase of the infectious cycle but that no significant induction of  
28  
29 223 protein expression occurred before 24h post-infection which corresponds to a late-phase protein  
30  
31 224 expression. Finally, the protein PahN encoded by a mid-phase transcribed gene showed also an  
32  
33 225 increased expression from 8h post-infection which is maintained during the mid to late-phase of the  
34  
35 226 replicative cycle. These data demonstrate that the temporal pattern of protein expression measured by  
36  
37 227 quantitative immunofluorescence of the 5 selected proteins Mscs/SctJ/CopN/SctW/PahN is similar to  
38  
39 228 their respective mRNA temporal expression measured by qRT-PCR. These data indicate that protein  
40  
41 229 and mRNA expression of various T3SS components are tightly coupled and that temporal  
42  
43 230 transcriptional expression analysis of multiple T3SS genes can be used to monitor the expression of  
44  
45 231 different T3SS components and thus to characterize its functionality during an infectious cycle.

## 232 **Discussion**

51  
52 233 Genome sequencing of multiple *Chlamydiales* bacteria belonging to different distant families have  
53  
54 234 demonstrated that despite marked differences in their genomic size and content, the T3SS loci  
55  
56 235 distributed in different clusters along the chromosomes exhibit a conserved sequence and genetic  
57  
58 236 organization (Collingro *et al.*, 2011a; Bertelli *et al.*, 2010; Greub *et al.*, 2009; Peters *et al.*, 2007).

1  
2  
3 237 Several studies have demonstrated that specific inhibition of T3SS with chemical compounds totally  
4  
5 238 inhibits bacterial growth in a dose dependent manner strongly indicating that this secretion system is  
6  
7 239 essential for the establishment of *Chlamydiales* replicative conditions (Bertelli *et al.*, 2010; Bailey *et*  
8  
9 240 *al.*, 2007; Muschiol *et al.*, 2006). The temporal expression of T3SS during a replicative cycle has only  
10  
11 241 been studied in *Chlamydiaceae* including *C. trachomatis*, *C. pneumoniae* and *C. psittaci*. In this study,  
12  
13 242 a complete characterization of the temporal expression of multiple T3SS components at the  
14  
15 243 transcriptional and protein level has been performed in *Parachlamydia acanthamoebae* replicating in  
16  
17 244 its natural host cell *Acanthamoeba castellanii*. This study is the first description of the T3SS  
18  
19 245 expression during the replicative cycle of a member of the *Chlamydiales* order not belonging to the  
20  
21 246 *Chlamydiaceae* family. The replicative cycle of *Parachlamydia* within *A. castellanii* was separated in  
22  
23 247 3 phases, early, mid and late. The early-phase is characterized by a lag-phase when EBs are  
24  
25 248 internalized in the host cell and differentiate into RBs. The mid-phase is characterized by exponential  
26  
27 249 bacterial replication. The late-phase is starting when bacteria enter stationary phase where RBs  
28  
29 250 redifferentiate into EBs which are then released in the extracellular milieu. This study showed that the  
30  
31 251 temporal transcriptional expression of multiple genes encoding for T3SS components could be  
32  
33 252 classified in 4 different temporal clusters depending on their pattern of expression during the early,  
34  
35 253 mid and late-phases of an infectious cycle. Classical western blotting being of limited value for  
36  
37 254 quantitative temporal assessment of protein expression of obligate intracellular bacteria, a new  
38  
39 255 quantitative immunofluorescence approach allowing accurate measurement of protein expression was  
40  
41 256 used in this study. The expression analysis of selected T3SS proteins encoded by genes belonging to  
42  
43 257 different temporal clusters showed that a similar temporal pattern of transcriptional and protein  
44  
45 258 expression was observed for each of these genes (*copB*, *mcsc*, *sctJ*, *pahN*, *sctW*).

46  
47  
48 259 Based on our experimental data, a model of temporal expression of T3SS during an infectious cycle  
49  
50 260 can be proposed (Figure 9). The T3SS is a multi-component complex machinery containing protein  
51  
52 261 with diverse functions and in varying quantities. A varying stoichiometric composition of the T3SS  
53  
54 262 could likely define the functionality of the apparatus. The levels of proteins in bacterial cells are  
55  
56 263 controlled by multiple mechanisms and are defined by both the rate of protein synthesis and protein  
57  
58  
59  
60

1  
2  
3 264 degradation, which are varying with the physiological status of the bacteria during a growth cycle. The  
4  
5 265 relative protein content of the T3SS in EBs is likely similar to the protein content observed during the  
6  
7 266 late-phase of the replicative cycle when RBs redifferentiate into EBs before cell lysis and bacterial  
8  
9 267 release in the extracellular milieu. During that time, the T3SS is likely not required for secretion of  
10  
11 268 bacterial effectors and maintained in a dormant state ready to be activated. Upon cell contact and  
12  
13 269 bacterial internalization of EBs, the T3SS is likely quickly activated to allow rapid secretion of  
14  
15 270 effector proteins to modulate host cell functions. Varying de novo rapid synthesis of T3SS  
16  
17 271 components depending of protein stability, quantity and functionality likely occurs during the critical  
18  
19 272 early-phase of bacterial infection to promote bacterial survival, differentiation, maturation and  
20  
21 273 initiation of replication. The subversion of host cell defense mechanisms has likely to be operated  
22  
23 274 during the early-phase of the infection to ensure bacterial evasion from the lytic pathway. Similarly, a  
24  
25 275 rapid modulation of host cell functions ensuring a fast maturation of the replicative vacuole is a pre-  
26  
27 276 request to trigger bacterial replication. Thus, the importance of a highly functional and efficient T3SS  
28  
29 277 during the early-phase of infection would likely confer a significant advantage for the intracellular  
30  
31 278 bacteria against the defense mechanisms of the host cell. In mid-phase, once the bacteria have  
32  
33 279 established conditions allowing efficient bacterial replication such as replicative vacuole maturation,  
34  
35 280 subversion of host cell defenses and establishment of systems allowing efficient scavenging of host  
36  
37 281 cell nutrients, the importance and the number of T3SS per bacteria are reduced or only maintained in  
38  
39 282 bacteria being in direct contact with the inclusion membrane. Finally, increased de novo synthesis of  
40  
41 283 some T3SS components in the late-phase trigger the shutdown of the apparatus (SctW) and the  
42  
43 284 formation of a silent T3SS in EBs ready to be rapidly activated when requested.

45 285 A significant similarity between the transcriptional expression units of *Parachlamydia* and *C.*  
46  
47 286 *trachomatis* was observed, suggesting that T3SSs sequences, genetic organization and transcriptional  
48  
49 287 expression units are highly conserved among *Chlamydiales* bacteria (Hefty and Stephens, 2007).  
50  
51 288 However, several studies indicate that the temporal expression of these transcriptional units may vary  
52  
53 289 among *Chlamydiales* bacteria (Beeckman *et al.*, 2008; Hefty and Stephens, 2007; Lugert *et al.*, 2004;  
54  
55 290 Slepkin *et al.*, 2003). Some discrepancies may originate from several issues including chlamydial  
56  
57 291 species specificities, growth kinetics differences, host cell lines and variation of the limit of detection  
58  
59  
60

1  
2  
3 292 of the molecular techniques used in the different experimental assets. The regulation of the T3SS  
4  
5 293 expression in *Chlamydiales* is poorly understood. T3SS genes and operons are preceded by predicted  
6  
7 294 *E. coli*  $\sigma$ 70-like promoter elements but no transcriptional regulators have yet been identified (Hefty  
8  
9 295 and Stephens, 2007). Similarly, the explanation of the separation of the *Chlamydiales* T3SS elements  
10  
11 296 in distinct genomic clusters and transcriptional units expressed in different temporal classes remained  
12  
13 297 to be determined. Transcriptional regulation of T3SS genes in other bacterial species such as *Yersinia*  
14  
15 298 and *Salmonella* is mainly controlled by AraC-like transcriptional activators whose activities are  
16  
17 299 regulated by several regulatory pathways responding to multiple environmental signals sensed during  
18  
19 300 the infection process (Francis *et al.*, 2002). No gene encoding for an AraC-like transcriptional  
20  
21 301 activators has been identified in *Chlamydiales* genomes, suggesting that *Chlamydiales* T3SSs are  
22  
23 302 regulated by a different mechanism. The absolute requirement of T3SS for chlamydial survival and  
24  
25 303 replication in host cells may suggest that T3SSs are controlled by the global regulatory network  
26  
27 304 system of *Chlamydiales* bacteria via various transcriptional regulators and/or alternative regulatory  
28  
29 305 systems. Recent data suggest that transcriptional expression of chlamydial T3SS operons is controlled  
30  
31 306 by the degree of DNA supercoiling that varies temporally during a developmental cycle (Case *et al.*,  
32  
33 307 2010). Thus, the differences of sensitivity of the promoters to alteration of DNA supercoiling may  
34  
35 308 define temporal transcriptional expression differences of T3SS operons and of other unrelated  
36  
37 309 chlamydial genes.

38  
39  
40 310 The *Chlamydiales* T3SS is rapidly activated upon contact with the host cell and remains probably  
41  
42 311 functional until bacterial detachment from the inclusion membrane and RBs conversion into EBs  
43  
44 312 (Fields, 2006; Clifton *et al.*, 2004; Fields *et al.*, 2003). Even though cell contact-dependent activation  
45  
46 313 of T3SS is conserved among bacteria (Hueck, 1998), the exact mechanism governing the activation in  
47  
48 314 *Chlamydiales* remains to be identified and marked differences compared to other bacterial species  
49  
50 315 T3SS could be observed considering the peculiar developmental cycle of *Chlamydiae*. For instance,  
51  
52 316 the *Chlamydiales* needle protein SctF contains cystein residues that are, like the proteins forming the  
53  
54 317 envelope, linked by disulfide bridges in EBs (Betts *et al.*, 2008b) indicating that a reduction of these  
55  
56 318 bonds could be required for a complete activation of the secretion. This hypothesis is supported by the  
57  
58  
59  
60

1  
2  
3 319 observation that the classical activation of T3SSs secretion obtained by Ca<sup>2+</sup> depletion did only  
4  
5 320 poorly stimulated the secretion of the Tarp effector from purified cell-free *C. trachomatis* EBs  
6  
7 321 (Jamison and Hackstadt, 2008).

8  
9  
10 322 Based on T3SS studies in other bacteria, some components of the chlamydial T3SS likely exhibit  
11  
12 323 secretion regulatory functions such as SctW (CopN), SctU and SctL. SctW contains domains similar to  
13  
14 324 *Yersinia* YopN and TyeA which are negative regulators of T3SS secretion (Joseph and Plano, 2007;  
15  
16 325 Goss *et al.*, 2004). The secretion of effector proteins by the T3SS is partially controlled by the  
17  
18 326 complex YopN/TyeA which interacts with the secretory apparatus to prevent secretion before  
19  
20 327 activation of the system upon detection of the right stimuli by the needle-tip complex (Joseph and  
21  
22 328 Plano, 2007). The breaking of the YopN/TyeA interaction triggered by the stimuli that activate the  
23  
24 329 T3SS induce the secretion of YopN, which render the apparatus operational for effectors secretion.  
25  
26 330 The homologous SctW protein of *Chlamydiales* could have a similar regulatory function in addition of  
27  
28 331 its secreted effector activity that trigger cell cycle arrest by altering the microtubule cytoskeleton  
29  
30 332 (Huang *et al.*, 2008; Fields and Hackstadt, 2000). The expression of SctW observed in late-phase of  
31  
32 333 the replicative cycle of *Parachlamydia* is compatible with the dual function of this protein. The  
33  
34 334 expression and the recruitment of SctW to the secretory apparatus in late-phase coincide with  
35  
36 335 deactivation of the T3SS and thus inhibition of secretion. During the early-phase of infection, SctW is  
37  
38 336 rapidly secreted which renders again the T3SS secretion competent.

39  
40  
41 337 The cleavage of the SctU *Yersinia* homolog YscU is required to permit secretion of effector proteins  
42  
43 338 likely by allowing the recruitment of the ATPase complex SctN/L to the apparatus (Riordan and  
44  
45 339 Schneewind, 2008). The transcriptional expression of the *sctU* gene is highly reduced in the mid-phase  
46  
47 340 of the replicative cycle of *Parachlamydia*, which suggest that once the T3SS apparatus is assembled  
48  
49 341 and activated, the requirement and the expression of the this protein is possibly decreased as observed  
50  
51 342 in this study, or that single SctU proteins might be shared by several T3SS apparatus when its  
52  
53 343 requirement decreases.  
54  
55  
56  
57  
58  
59  
60

1  
2  
3 344 Regulation of the T3SS during the replicative cycle might be operated through the controlled temporal  
4  
5 345 expression of some components required to initiate protein-protein interactions or functionality. For  
6  
7 346 instance, studies on the *Yersinia* T3SS indicate that the assembly of the cytosolic complex consisting  
8  
9 347 of the ATPase SctN, the interacting protein SctL and the C ring component SctQ require the presence  
10  
11 348 of all of its components (Diepold *et al.*, 2010; Jackson and Plano, 2000). Thus, in *Parachlamydia*, the  
12  
13 349 late-phase cycle expressed proteins SctN and SctQ would not be active until the early-phase  
14  
15 350 expression of maximal amounts of SctL initiates or increases the early formation of the  
16  
17 351 SctN/SctL/SctQ complex, triggering its docking onto the IM ring and the subsequent full activation of  
18  
19 352 the T3SS secretion system. Similarly, the early expression of the multiple cargo secretion chaperone  
20  
21 353 Mcsc would initiate or increase a protein-protein interaction hub consisting of Mcsc-effector-SctQ  
22  
23 354 complexes and activation of T3SS-dependent effectors secretion.

24  
25  
26 355 The CopB protein identified in *Parachlamydia* is poorly homologous to the translocator proteins  
27  
28 356 CopB and CopB2 of *Chlamydiaceae* bacteria (Chellas-Gery *et al.*, 2011) . Similar to *setU*, the  
29  
30 357 expression of CopB is reduced during the mid-phase. Even though no sequence homologies are  
31  
32 358 observed, CopB of *Parachlamydia* exhibit more similarities with the predicted secondary structures of  
33  
34 359 the *C. trachomatis* CopB2 than with CopB (data not shown). In addition, no co-localisation of CopB  
35  
36 360 with the inclusion membrane of *Parachlamydia* has been observed in this study suggesting that this  
37  
38 361 protein is possibly secreted in the host cell cytoplasm similarly to CopB2 of *C. trachomatis* (Chellas-  
39  
40 362 Gery *et al.*, 2011).

41  
42  
43 363 In conclusion, the differential temporal expression of T3SS components during the replicative cycle  
44  
45 364 of *Parachlamydia* suggests that the maximal expression and activation of T3SS injectisomes occurs  
46  
47 365 during the early to mid-phase of the infectious cycle, which corresponds to a critical phase during  
48  
49 366 which the intracellular bacterium has to evade and/or block lytic effectors of the amoebal host cell, to  
50  
51 367 differentiate from EBs to RBs and to modulate the maturation of its replicative vacuole to create  
52  
53 368 replicative condition able to sustain efficient bacterial replication. Based on several studies mainly  
54  
55 369 performed in other bacteria than *Chlamydiales*, the functions of several T3SS components are well  
56  
57 370 described whereas for other components, no functionality has yet been attributed. In addition of a  
58  
59  
60

1  
2  
3 371 described enzymatic, regulatory or structural function, a temporal activity remains to be characterized  
4  
5 372 for many proteins that compose the chlamydial T3SS machinery. The T3SS machinery is likely a  
6  
7 373 dynamic structure which can fluctuate during a replicative cycle to modulate its functionality. The  
8  
9 374 expression of each component of the T3SS during the replicative cycle depends of several molecular  
10  
11 375 criteria including function, activity, stoichiometric ratio, stability and turnover of each protein. In  
12  
13 376 addition, some proteins might be shared between different apparatus of the cell. Finally, recent data  
14  
15 377 strongly suggest that unlike other described bacterial species, the *Chlamydiales* T3SS is likely deeply  
16  
17 378 involved in additional roles than solely protein secretion and translocation (Peters *et al.*, 2007). For  
18  
19 379 instance, the attachment to inclusion membranes and the differentiation of RBs into EBs may be  
20  
21 380 controlled by the T3SS. Thus, differential temporal expression of various components of the  
22  
23 381 chlamydial T3SS may be required to modulate these multiple regulatory activities.

## 26 382 **Experimental procedures**

27  
28  
29 383 **Bacterial strain.** *P. acanthamoebae* strain Hall's coccus were grown at 32 °C within *Acanthamoeba*  
30  
31 384 *castellanii* in 75-cm<sup>2</sup> cell culture flasks (Corning, New-York, USA) with 30 ml of peptone-yeast  
32  
33 385 extract-glucose (PYG) broth (Greub and Raoult, 2002). After 5 days of incubation, cultures were  
34  
35 386 harvested and the broth was filtered through a 5µm pore to eliminate both amoebal trophozoites and  
36  
37 387 cysts and to collect bacteria in the flow through. *A. castellanii* ATCC 30010 was cultured in 75-cm<sup>2</sup>  
38  
39 388 cell culture flasks at 25°C.

40  
41  
42 389 **Infection procedure.** Amoebae harvested from 24h fresh culture were centrifuged at 200 × *g* for 5  
43  
44 390 min, resuspended in RPMI-HEPES supplemented with 200 mM L-glutamine (Gibco-BRL, Life  
45  
46 391 Technologies, Paisley, Scotland) and 10% fetal calf serum (Gibco-BRL). Then, 10<sup>5</sup> amoeba cells/ml  
47  
48 392 were incubated for 2h at 25 °C in 24-well cell culture plates (Corning). Non-adherent cells were  
49  
50 393 washed and the remaining adherent cells were incubated for 16h at 25°C.

51  
52 394 The amount of bacteria after 5 days of amoebal co-culture was equal to about 10<sup>8</sup> cells per ml as  
53  
54 395 measured by quantitative PCR of the 16S rDNA. Host cell lysis assay following infection of *A.*

1  
2  
3 396 *castellanii* with limiting serial dilution of a bacterial filtrate confirmed that most collected bacteria are  
4  
5 397 living cells.

6  
7 398 Wells containing  $10^5$  amoebae were infected with a  $10^6$  bacteria/ml suspension corresponding to a  
8  
9 399 multiplicity of infection (MOI) of about 10. Plates were centrifuged at  $1790 \times g$  for 10 min at room  
10  
11 400 temperature. After 30 min of incubation at  $32^\circ\text{C}$ , amoebal cells were washed with RPMI-HEPES and  
12  
13 401 further incubated for different periods at  $32^\circ\text{C}$  in RPMI-HEPES supplemented with 200 mM L-  
14  
15 402 glutamine and 10% fetal calf serum.

16  
17 403 **Confocal microscopy.** Infected amoebae were washed with PBS, fixed with ice-cold methanol for 4  
18  
19 404 min. Cells were then washed three times with PBS and were then blocked and permeabilised for 1h in  
20  
21 405 a blocking solution (PBS/0.1% Saponin/10% fetal calf serum). Coverslips were incubated with  
22  
23 406 primary mouse antisera directed against different specific proteins (CopB, SycD1, Mcsc, SctW, SctJ,  
24  
25 407 PahN) or against total whole cells of *Parachlamydia* for 1h at room temperature in blocking solution.  
26  
27 408 After washing three times with PBS/0.1% saponin, coverslips were incubated for 1h with secondary  
28  
29 409 anti-mouse antibodies in blocking solution containing concanavalin A (Invitrogen, Basel, Switzerland)  
30  
31 410 and DAPI (dilactate, D3571, Molecular Probes, OR, USA) to counterstain amoebae and label DNA,  
32  
33 411 respectively. After two washing in PBS/0.1% saponin, two in PBS and one with deionised water, the  
34  
35 412 coverslips were mounted onto glass slides using Mowiol (Sigma-Aldrich, MO, USA). Cells were  
36  
37 413 observed on a confocal fluorescence microscope (Zeiss LSM710 Meta, Jena, Germany). Files were  
38  
39 414 analysed using Image J for microscopy ([www.macbiophotonics.com](http://www.macbiophotonics.com)) softwares. All the assays were  
40  
41 415 performed at least in triplicate.

42  
43 416 **Quantitative reverse transcription polymerase chain reaction (qRT-PCR).** Amoebae were  
44  
45 417 infected in 24-wells plates as described before. Samples were harvested at different times  
46  
47 418 post-infection by scraping amoeba cells from the well surface and by resuspending the  
48  
49 419 samples in RNeasy Protect Bacteria reagent (Qiagen GmbH, Germany). Total RNA was extracted  
50  
51 420 using the RNeasy Plus Mini Kit (Qiagen GmbH, Germany) as described by the manufacturer.  
52  
53 421 The RNA samples were treated with the DNA-free kit (Ambion, Applied Biosystems,  
54  
55 422 California, USA) to remove contaminating DNA from the RNA preparation.  
56  
57  
58  
59  
60

1  
2  
3 423 The analysis of mRNA quantification was performed by a one step reverse transcription polymerase  
4 424 chain reaction using the One step MESA GREEN qRT-PCR MasterMix Plus for SYBR® assay  
5 425 (Eurogentec, Seraing, Belgium). The design of the specific primers listed in table 1 was done with the  
6  
7 426 Primer3plus software (<http://primer3.sourceforge.net/webif.php>). The qRT-PCR assay was performed  
8  
9 427 in a total volume of 20 µl with 10 µl of 2x reaction buffer, 100nM forward primer, 100nM reverse  
10  
11 428 primer, 0.25U/µl Euroscript reverse transcriptase, 0.1U/µl RNase inhibitor and RNase-free water. The  
12  
13 429 thermocycling conditions were set up as follow: (i) reverse transcription, 30min, 48°C, (ii) Meteor *Taq*  
14  
15 430 activation and Euroscript inactivation, 5min, 95°C, (iii) 40 cycles, 15sec, 95°C, 1min, 60°C, (iv) melt  
16  
17 431 curve analysis, temperature increment of 0.3% from 60 to 95°C. The analysis of the 16S rRNA was  
18  
19 432 used as an internal control to normalize the quantification of every specific mRNA collected at  
20  
21 433 different times during an infectious cycle. The results are presented as a relative quantification taking  
22  
23 434 samples at time 0 (EBs) as a reference of 1. Water was used as a negative control and the qRT-PCR  
24  
25 435 reaction without reverse transcriptase was used as a control to measure DNA contamination in the  
26  
27 436 extracted RNA samples. All measurements were performed at least in triplicates.

28  
29  
30  
31 437 **Protein purification and generation of antisera.** *P. acanthamoebae sctJ*, *sctW*, *copB*, *mcsc*, *pahN*  
32  
33 438 and *sycD* (*scc2*) ORFs were amplified from purified *P. acanthamoebae* genomic DNA using primers  
34  
35 439 listed in table 2 using the high fidelity Phusion polymerase (Finnzymes, Espoo, Finland). Using the  
36  
37 440 Champion pET directional TOPO Expression Kits (Invitrogen), *sctJ* and *mcsc* were cloned in frame  
38  
39 441 with a N-terminal and C-terminal peptide containing a polyhistidine (6xHis) tag to generate the  
40  
41 442 plasmids pET200/D-TOPO-*sctJ* and pET101/D-TOPO-*mcsc*, respectively (Table 2). The four bases  
42  
43 443 CACC were added to the forward primers to allow directional in-frame cloning of the PCR fragments  
44  
45 444 into plasmids pET200/D-TOPO and pET101/D-TOPO. Following digestion of the PCR amplicons and  
46  
47 445 the plasmids with *NcoI*/*HindIII*, *copB* (nt 1-960) and *pahN* were ligated into the plasmid  
48  
49 446 pBADmycHis (Invitrogen) to generate the plasmids pBADmycHis-*copB* and pBADmycHis-*pahN*  
50  
51 447 encoding for C-terminal polyhistidine tag (6xHis) recombinant proteins. Similarly, *copN* and *scc2*  
52  
53 448 amplicons and the plasmid pET28a were digested with *NdeI*/*BamHI* to generate by ligation the  
54  
55 449 plasmids pET28a-*copN* and pET28a-*scc2* encoding for N-terminal polyhistidine tag recombinant  
56  
57 450 proteins. The proteins were expressed in BL21 star (DE3) *E. coli* strains following 0.5mM IPTG  
58  
59  
60

1  
2  
3 451 (pET200/D-TOPO-*sctJ* / pET101/D-TOPO-*mcsc* / pET28a-*copN* / pET28a-*scc2*) induction at 37°C or  
4  
5 452 in TOP10 *E. coli* strains following 0.02% arabinose (pBADmycHis-*copB* / pBADmycHis-*pahN* )  
6  
7 453 induction at 37°C. The BL21 and TOP10 *E.coli* strains expressing the protein of interest were lysed  
8  
9 454 with the FastBreak cell lysis solution (Promega) and recombinant His-tagged proteins were purified in  
10  
11 455 native or denaturing conditions using the MagneHis protein purification system (Promega) according  
12  
13 456 to the manufacturer's recommendation. Purified recombinant His-tagged proteins were used to  
14  
15 457 conduct mouse immunization programs at the Eurogentec animal facility (Eurogentec, Seraing,  
16  
17 458 Belgium) to elicit the production of specific mouse antisera.

18  
19 459 **Western blot.** For Immunoblot analysis, protein samples were separated by SDS-PAGE, transferred  
20  
21 460 to 0.45 µm nitrocellulose membranes and blocked with 5% non-fat powder milk in TBST (50mM  
22  
23 461 Tris-Base, 150mM NaCl, 0.2% Tween pH7.4). The nitrocellulose membranes were incubated with  
24  
25 462 mouse primary antibodies (anti-SctJ, SctW, CopB, Mcsc, SctF) diluted in 0.5% milk-TBST, washed 3  
26  
27 463 times, incubated with secondary antibody conjugated to horseradish peroxidase diluted in 0.5% milk-  
28  
29 464 TBST and detected by chemiluminescence. The density of the bands on western blots was measured  
30  
31 465 with the gel analysis method of the ImageJ software as described by Luke Miller  
32  
33 466 (<http://lukemiller.org/index.php/2010/11/analyzing-gels-and-western-blots-with-image-j/>). Western  
34  
35 467 blot have been done at least in triplicates for each analyzed proteins.

36  
37 468 **Quantitative immunofluorescence.** Proteins were labeled by immunofluorescence staining with  
38  
39 469 specific mouse polyclonal antibodies as described in confocal microscopy. A series of images of  
40  
41 470 multiple focal planes covering the entire thickness of the sample were collected by z-stack confocal  
42  
43 471 microscopy. Using the ImageJ software, a Z-projection composed of the summing of the slices was  
44  
45 472 generated. The region of interest (ROI) including only the signal of intensity emitted by the bacteria  
46  
47 473 was defined by applying a median filter (2x2.0 pixels) and by adjusting the Isodata threshold setup. A  
48  
49 474 histogram of the ROI composed of the signal intensity on the x-axis and of the frequency on the y-axis  
50  
51 475 was generated. A mean value and a standard deviation of the histogram of the frequency distribution  
52  
53 476 of fluorescence intensity were also generated. The results were then exported and analyzed using  
54  
55 477 GraphPad Prism version 5.00 for Windows (GraphPad Software, San Diego California USA). The  
56  
57 478 signal intensity for each frequency was normalized by using a value of 100 for the highest intensity.  
58  
59  
60

479 Several images from one experiment performed at least in triplicates have been analyzed for each  
480 protein.

481

## 482 References

- 483 Bailey, L., Gylfe, A., Sundin, C., Muschiol, S., Elofsson, M., Nordstrom, P., *et al* (2007) Small  
484 molecule inhibitors of type III secretion in *Yersinia* block the *Chlamydia pneumoniae* infection cycle.  
485 *FEBS Lett.* **581**: 587-595.
- 486 Bannantine, J.P., Griffiths, R.S., Viratyosin, W., Brown, W.J. and Rockey, D.D. (2000) A secondary  
487 structure motif predictive of protein localization to the chlamydial inclusion membrane. *Cell*  
488 *Microbiol.* **2**: 35-47.
- 489 Beeckman, D.S. and Vanrompay, D.C. (2010) Bacterial secretion systems with an emphasis on the  
490 chlamydial Type III secretion system. *Curr Issues Mol Biol.* **12**: 17-41.
- 491 Beeckman, D.S., Geens, T., Timmermans, J.P., Van Oostveldt, P. and Vanrompay, D.C. (2008)  
492 Identification and characterization of a type III secretion system in *Chlamydia psittaci*. *Veterinary*  
493 *research.* **39**: 27.
- 494 Bertelli, C., Collyn, F., Croxatto, A., Ruckert, C., Polkinghorne, A., Kebbi-Beghdadi, C., *et al* (2010)  
495 The *Waddlia* genome: a window into chlamydial biology. *PLoS One.* **5**: e10890.
- 496 Betts-Hampikian, H.J. and Fields, K.A. (2010) The Chlamydial Type III Secretion Mechanism:  
497 Revealing Cracks in a Tough Nut. *Frontiers in microbiology.* **1**: 114.
- 498 Betts, H.J., Twigg, L.E., Sal, M.S., Wyrick, P.B. and Fields, K.A. (2008a) Bioinformatic and  
499 biochemical evidence for the identification of the type III secretion system needle protein of  
500 *Chlamydia trachomatis*. *J Bacteriol.* **190**: 1680-1690.
- 501 Betts, H.J., Twigg, L.E., Sal, M.S., Wyrick, P.B. and Fields, K.A. (2008b) Bioinformatic and  
502 biochemical evidence for the identification of the type III secretion system needle protein of  
503 *Chlamydia trachomatis*. *Journal of bacteriology.* **190**: 1680-1690.
- 504 Case, E.D., Peterson, E.M. and Tan, M. (2010) Promoters for *Chlamydia* type III secretion genes show  
505 a differential response to DNA supercoiling that correlates with temporal expression pattern. *J*  
506 *Bacteriol.* **192**: 2569-2574.
- 507 Casson, N., Medico, N., Bille, J. and Greub, G. (2006) *Parachlamydia acanthamoebae* enters and  
508 multiplies within pneumocytes and lung fibroblasts. *Microbes Infect.* **8**: 1294-1300.
- 509 Casson, N., Entenza, J.M., Borel, N., Pospischil, A. and Greub, G. (2008) Murine model of pneumonia  
510 caused by *Parachlamydia acanthamoebae*. *Microbial pathogenesis.* **45**: 92-97.
- 511 Chellas-Gery, B., Wolf, K., Tisoncik, J., Hackstadt, T. and Fields, K.A. (2011) Biochemical and  
512 localization analyses of putative type III secretion translocator proteins CopB and CopB2 of  
513 *Chlamydia trachomatis* reveal significant distinctions. *Infect Immun.* **79**: 3036-3045.
- 514 Clifton, D.R., Fields, K.A., Grieshaber, S.S., Dooley, C.A., Fischer, E.R., Mead, D.J., *et al* (2004) A  
515 chlamydial type III translocated protein is tyrosine-phosphorylated at the site of entry and associated  
516 with recruitment of actin. *Proc Natl Acad Sci U S A.* **101**: 10166-10171.
- 517 Coburn, B., Sekirov, I. and Finlay, B.B. (2007) Type III secretion systems and disease. *Clin Microbiol*  
518 *Rev.* **20**: 535-549.
- 519 Collingro, A., Tischler, P., Weinmaier, T., Penz, T., Heinz, E., Brunham, R.C., *et al* (2011a) Unity in  
520 Variety - the Pan-Genome of the Chlamydiae. *Molecular biology and evolution.*
- 521 Collingro, A., Tischler, P., Weinmaier, T., Penz, T., Heinz, E., Brunham, R.C., *et al* (2011b) Unity in  
522 variety--the pan-genome of the Chlamydiae. *Mol Biol Evol.* **28**: 3253-3270.
- 523 Cornelis, G.R. (2002) The *Yersinia Ysc-Yop* 'type III' weaponry. *Nat Rev Mol Cell Biol.* **3**: 742-752.
- 524 Corsaro, D. and Greub, G. (2006) Pathogenic potential of novel Chlamydiae and diagnostic  
525 approaches to infections due to these obligate intracellular bacteria. *Clin Microbiol Rev.* **19**: 283-297.
- 526 Diepold, A., Amstutz, M., Abel, S., Sorg, I., Jenal, U. and Cornelis, G.R. (2010) Deciphering the  
527 assembly of the *Yersinia* type III secretion injectisome. *The EMBO journal.* **29**: 1928-1940.

- 1  
2  
3 528 Fields, K.A. and Hackstadt, T. (2000) Evidence for the secretion of Chlamydia trachomatis CopN by a  
4 529 type III secretion mechanism. *Mol Microbiol.* **38**: 1048-1060.
- 5 530 Fields, K.A., Mead, D.J., Dooley, C.A. and Hackstadt, T. (2003) Chlamydia trachomatis type III  
6 531 secretion: evidence for a functional apparatus during early-cycle development. *Mol Microbiol.* **48**:  
7 532 671-683.
- 8 533 Fields, K.A., Hackstadt, T. (2006) The Chlamydia Type III secretion system: Structure and  
9 534 implications for pathogenesis. In *Chlamydia: Genomics and Pathogenesis*. Wyrick, P.M.B.a.P.B.  
10 535 (ed.): Horizon Bioscience, pp. 219-233.
- 11 536 Francis, M.S., Wolf-Watz, H. and Forsberg, A. (2002) Regulation of type III secretion systems. *Curr*  
12 537 *Opin Microbiol.* **5**: 166-172.
- 13 538 Goss, J.W., Sorg, J.A., Ramamurthi, K.S., Ton-That, H. and Schneewind, O. (2004) The secretion  
14 539 signal of YopN, a regulatory protein of the Yersinia enterocolitica type III secretion pathway. *Journal*  
15 540 *of bacteriology.* **186**: 6320-6324.
- 16 541 Greub, G. (2009) Parachlamydia acanthamoebae, an emerging agent of pneumonia. *Clin Microbiol*  
17 542 *Infect.* **15**: 18-28.
- 18 543 Greub, G. and Raoult, D. (2002) Crescent bodies of Parachlamydia acanthamoeba and its life cycle  
19 544 within Acanthamoeba polyphaga: an electron micrograph study. *Appl Environ Microbiol.* **68**: 3076-  
20 545 3084.
- 21 546 Greub, G. and Raoult, D. (2003) History of the ADP/ATP-translocase-encoding gene, a parasitism  
22 547 gene transferred from a Chlamydiales ancestor to plants 1 billion years ago. *Appl Environ Microbiol.*  
23 548 **69**: 5530-5535.
- 24 549 Greub, G. and Raoult, D. (2004) Microorganisms resistant to free-living amoebae. *Clin Microbiol Rev.*  
25 550 **17**: 413-433.
- 26 551 Greub, G., Mege, J.L. and Raoult, D. (2003a) Parachlamydia acanthamoebae enters and multiplies  
27 552 within human macrophages and induces their apoptosis [corrected]. *Infect Immun.* **71**: 5979-5985.
- 28 553 Greub, G., Berger, P., Papazian, L. and Raoult, D. (2003b) Parachlamydiaceae as rare agents of  
29 554 pneumonia. *Emerg Infect Dis.* **9**: 755-756.
- 30 555 Greub, G., Desnues, B., Raoult, D. and Mege, J.L. (2005a) Lack of microbicidal response in human  
31 556 macrophages infected with Parachlamydia acanthamoebae. *Microbes Infect.* **7**: 714-719.
- 32 557 Greub, G., Boyadjiev, I., La Scola, B., Raoult, D. and Martin, C. (2003c) Serological hint suggesting  
33 558 that Parachlamydiaceae are agents of pneumonia in polytraumatized intensive care patients. *Ann N Y*  
34 559 *Acad Sci.* **990**: 311-319.
- 35 560 Greub, G., Mege, J.L., Gorvel, J.P., Raoult, D. and Meresse, S. (2005b) Intracellular trafficking of  
36 561 Parachlamydia acanthamoebae. *Cell Microbiol.* **7**: 581-589.
- 37 562 Greub, G., Kebbi-Beghdadi, C., Bertelli, C., Collyn, F., Riederer, B.M., Yersin, C., *et al* (2009) High  
38 563 throughput sequencing and proteomics to identify immunogenic proteins of a new pathogen: the dirty  
39 564 genome approach. *PLoS One.* **4**: e8423.
- 40 565 Hefty, P.S. and Stephens, R.S. (2007) Chlamydial type III secretion system is encoded on ten operons  
41 566 preceded by sigma 70-like promoter elements. *J Bacteriol.* **189**: 198-206.
- 42 567 Horn, M., Collingro, A., Schmitz-Esser, S., Beier, C.L., Purkhold, U., Fartmann, B., *et al* (2004)  
43 568 Illuminating the evolutionary history of chlamydiae. *Science.* **304**: 728-730.
- 44 569 Huang, J., Lesser, C.F. and Lory, S. (2008) The essential role of the CopN protein in Chlamydia  
45 570 pneumoniae intracellular growth. *Nature.* **456**: 112-115.
- 46 571 Hueck, C.J. (1998) Type III protein secretion systems in bacterial pathogens of animals and plants.  
47 572 *Microbiol Mol Biol Rev.* **62**: 379-433.
- 48 573 Jackson, M.W. and Plano, G.V. (2000) Interactions between type III secretion apparatus components  
49 574 from Yersinia pestis detected using the yeast two-hybrid system. *FEMS microbiology letters.* **186**: 85-  
50 575 90.
- 51 576 Jamison, W.P. and Hackstadt, T. (2008) Induction of type III secretion by cell-free Chlamydia  
52 577 trachomatis elementary bodies. *Microb Pathog.* **45**: 435-440.
- 53 578 Joseph, S.S. and Plano, G.V. (2007) Identification of TyeA residues required to interact with YopN  
54 579 and to regulate Yop secretion. *Advances in experimental medicine and biology.* **603**: 235-245.
- 55 580 Lamoth, F. and Greub, G. (2009) Amoebal pathogens as emerging causal agents of pneumonia. *FEMS*  
56 581 *Microbiol Rev.*

- 1  
2  
3 582 Lugert, R., Kuhns, M., Polch, T. and Gross, U. (2004) Expression and localization of type III  
4 583 secretion-related proteins of *Chlamydia pneumoniae*. *Med Microbiol Immunol.* **193**: 163-171.  
5 584 Mota, L.J. and Cornelis, G.R. (2005) The bacterial injection kit: type III secretion systems. *Ann Med.*  
6 585 **37**: 234-249.  
7 586 Muschiol, S., Bailey, L., Gylfe, A., Sundin, C., Hultenby, K., Bergstrom, S., *et al* (2006) A small-  
8 587 molecule inhibitor of type III secretion inhibits different stages of the infectious cycle of *Chlamydia*  
9 588 *trachomatis*. *Proc Natl Acad Sci U S A.* **103**: 14566-14571.  
10 589 Noursadeghi, M., Tsang, J., Haustein, T., Miller, R.F., Chain, B.M. and Katz, D.R. (2008)  
11 590 Quantitative imaging assay for NF-kappaB nuclear translocation in primary human macrophages.  
12 591 *Journal of immunological methods.* **329**: 194-200.  
13 592 Peters, J., Wilson, D.P., Myers, G., Timms, P. and Bavoil, P.M. (2007) Type III secretion a la  
14 593 *Chlamydia*. *Trends Microbiol.* **15**: 241-251.  
15 594 Riordan, K.E. and Schneewind, O. (2008) YscU cleavage and the assembly of *Yersinia* type III  
16 595 secretion machine complexes. *Mol Microbiol.* **68**: 1485-1501.  
17 596 Slepkenin, A., Motin, V., de la Maza, L.M. and Peterson, E.M. (2003) Temporal expression of type III  
18 597 secretion genes of *Chlamydia pneumoniae*. *Infect Immun.* **71**: 2555-2562.  
19 598 Subtil, A., Delevoye, C., Balana, M.E., Tastevin, L., Perrinet, S. and Dautry-Varsat, A. (2005) A  
20 599 directed screen for chlamydial proteins secreted by a type III mechanism identifies a translocated  
21 600 protein and numerous other new candidates. *Mol Microbiol.* **56**: 1636-1647.

22  
23 601  
24  
25  
26  
27  
28  
29  
30  
31  
32  
33  
34  
35  
36  
37  
38  
39  
40  
41  
42  
43  
44  
45  
46  
47  
48  
49  
50  
51  
52  
53  
54  
55  
56  
57  
58  
59  
60

602 **Tables**603 **Table 1.** List of primers used in qRT-PCR

Name	Sequence	T <sub>m</sub>	Product Size
qRT-PCR-16S-F	TGACGATGCGACGCCGTGTG	60.38	
qRT-PCR-16S-R	GCAGCTGCTGGCACGGAGTT	60.25	142
qRT-PCR-sycD#1-F	AGGGCTTGCTCCGAAAGACCTCA	59.87	
qRT-PCR-sycD#1-R	ACAGGCCGCCAATCCCATCG	59.48	175
qRT-PCR-copB-F	TAGGCGCGGGTGCAGTTTG	59.97	
qRT-PCR-copB-R	CAATGCTGGCGGCCCTGGAA	59.97	167
qRT-PCR-sycD#2-F	GCAAGCCATGGGCCTTAGCGA	59.78	
qRT-PCR-sycD#2-R	TCGACGCTGCAAGTCCGAGTG	59.47	161
qRT-PCR-setJ-F	GCTCGGCAAGACCCGCTGA	59.7	
qRT-PCR-setJ-R	AGGCGACGCAAGCCATGTGC	60.38	144
qRT-PCR-setL-F	GCTTCAAAGCCTTCTTTTGGAGCGGC	60.01	
qRT-PCR-setL-R	GCGCTAGCTCTAAGGTCTGTTCTG	59.46	161
qRT-PCR-setT-F	GTGCGGCAAAACACGCGCTC	60.64	
qRT-PCR-setT-R	ACAGTGCCTTGCCACTGGAG	59.92	119
qRT-PCR-setC-F	TGCTCCTGCTGGTGGAGTCGT	59.84	
qRT-PCR-setC-R	TGCAGTAGGCTGCGGCACAA	59.27	139
qRT-PCR-pkn5-F	AAAGCGGGGATCGCCTGAGC	59.49	
qRT-PCR-pkn5-R	CCCTCCTCCCGGACGTCAA	59.61	170
qRT-PCR-setQ-F	TTGGGAAGCGTTTGCGCAGC	59.37	
qRT-PCR-setQ-R	CCCACCAAACGGGACCTTCAATCG	60	170
qRT-PCR-setF-F	GCGCGAAAGCCAAACTGCTTGA	59.44	
qRT-PCR-setF-R	AGTTCGCTGCACTGATAACCGCTG	59.83	138
qRT-PCR-setD-F	CCGGAAGAAGAGGACGCCGC	59.84	
qRT-PCR-setD-R	GGTGCGCCATCTCAGCGACA	60.05	143
qRT-PCR-setW-F	ACCGCGGAGCAAGCGGAAAG	60.32	
qRT-PCR-setW-R	GCGCTGCGCAGAAAGTGGC	60.11	111
qRT-PCR-setU-F	ACGTGCTCAGGCAGTTGTCACG	59.93	
qRT-PCR-setU-R	CGCTCAGCTAGGGCGTCTTCG	59.67	117
qRT-PCR_Mesc-F	TGGCACGTTTGCTTCACCTCATCA	59.35	
qRT-PCR_Mesc-R	TGGCGGGGATGAGAAGGCGG	60.95	102
qRT-PCR_setE-F	AGCGGATCCTGTGAAAATGCGGG	59.81	
qRT-PCR_setE-R	TTCGCGAGATCACTTTTAGCATGGATGT	59.01	158
qRT-PCR_setG-F	ACTTCCCTTGCTAATCGAGGCTGGT	59.95	
qRT-PCR_setG-R	TGCCCGGGACTCATCGCTTCT	59.98	103
qRT-PCR_setN-F	AGCGCGTCGGCATTTTGCG	60.11	
qRT-PCR_setN-R	GTCACGAAGCTCACGCCCC	60.04	128
qRT-PCR_setV-F	GATCACCAAGGGTGCGGAACGG	60.05	
qRT-PCR_setV-R	AGCGCGCATATCGGCGTCAA	59.91	100
qRT-PCR-pahN-F	GCCCCGTGTGGAATCTGCACC	60.31	
qRT-PCR-pahN-R	AGCAAGCAAACAACCTCACAGGCCA	59.76	124
qRT-PCR_gyrB-F	CCTGCGTATGCGCCCTTCCA	59.8	
qRT-PCR_gyrB-R	TGGTGCCGCGTTTGGTGGTT	60	135
qRT-PCR_hsp60-1-F	CAAGCACGAAAACATGGGCGCT	59.2	

qRT-PCR	<b>hsp60-1-R</b>	GCTCCAGCTGCGACATTGCG	59.3	141
qRT-PCR	<b>secY-F</b>	TGGGGAAGCGGCAAAGCGAA	59.6	
qRT-PCR	<b>secY-R</b>	TCACCAGCGACGATACCTGGCTT	60	135
qRT-PCR	<b>rpoB-F</b>	ACGGCGCTGAAAGGGTTGTTGT	59.8	
qRT-PCR	<b>rpoB-R</b>	TCCGCGCATGTGGCGTTCTT	60	80
qRT-PCR	<b>hc1-F</b>	GGCACAAAAGGCCGCGCAA	59.9	
qRT-PCR	<b>hc1-R</b>	AGCAGCATGTTTAGGCGCAGCA	59.9	87

604

605

T<sub>m</sub> calculation: thermodynamic parameters and salt correction formula: SantaLucia JR, 1998

**Table 2.** Cloning primers and plasmids

primers	sequences	plasmids	His-tag position	Comments
sctJ-For	<b>CACCGAATCGCGAAAACGATTG</b>			
sctJ-Rev	TTAAGATTCTTTAGCCACAATGATTGAC	pET200/D-TOPO	N-terminal	direct PCR product TOPO directional cloning
mesc-For	<b>CACCATGGTAAAATTAAGCTAGATAGAATCATCG</b>			
mesc-Rev	AAGGGTATGTTTTTTTTCTTCTTGIG	pET101/D-TOPO	C-terminal	direct PCR product TOPO directional cloning
copB-For (NcoI)	GGTGGT <b>CCATGG</b> TGAATGAATTTAATATTTTCATCACAGGGACA			
copB-Rev (HindIII)	GGTGGT <b>AAGCTT</b> TAAATTTCTGTTGGCTCGCTGTTC	pBADmycHis	C-terminal	subcloning nt 1-960
copN-For (NdeI)	GGTGGT <b>CATATG</b> CCCGATTGGAATATCCAACAAG			
copN-Rev (BamHI)	GGTGGT <b>GGATCC</b> TTATTCTTTATCTTCCTCTTCTTCCIGTT	pET28a	N-terminal	
scc2-For (NdeI)	GGTGGT <b>CATATG</b> AAAGGTGAACAAAGTCAAATCAAAAAGG			
scc2-Rev (BamHI)	GGTGGT <b>GGATCC</b> CTATGAAATCGGTTGATTTTCTTCAGC	pET28a	N-terminal	
pahN-For (NcoI)	GGTGGT <b>CCATGG</b> CTATAAGTTTATATTCAAATCAACAACC			
pahN-Rev (EcoRI)	GGTGGT <b>GAATTC</b> GTATTAGACGTTGCAGGTTTTTCTTC	pBADmycHis	C-terminal	

Primers: The restriction enzymes used to digest and clone the PCR products in the plasmids pBADmycHis and pET28a are indicated in brackets. Sequences: the restriction enzymes cleavage sequences are indicated in bold and underlined. The four bases CACC added to the forward primers to allow directional in-frame cloning of the PCR fragments into plasmids pET101/D-TOPO and pET200/D-TOPO are indicated in bold.

1  
2  
3 611 **Figure legends**  
4  
5

6 612 **Fig 1.** Temporal characterization of the replicative cycle. (A) *Acanthamoeba castellanii* were infected  
7  
8 613 with *Parachlamydia acanthamoebae* at a MOI of 10 to obtain an amoebal infectious rate of nearly  
9  
10 614 100% ensuring that only a single infectious cycle occurred in every experiment. Samples were  
11  
12 615 collected at the indicated times post-infection to cover the complete replicative cycle. Bacteria (green)  
13  
14 616 were labeled by immunofluorescence using specific mouse anti-*P. acanthamoebae* polyclonal  
15  
16 617 antibodies. *A. castellanii* (red) were stained with concanavalin A. An average of 2-5 infectious  
17  
18 618 particles per amoebal cell were observed 1h post-infection. Internalization and differentiation of EBs  
19  
20 619 into RBs occurred during the 5 first hours of the infection. Replicating RBs located in bacterial  
21  
22 620 inclusions were observed from 8 to 24h post-infection. Redifferentiation of RBs into EBs occurred  
23  
24 621 between 24-48h post-infection. Finally cell lysis and extrusion of infectious EBs from host cells were  
25  
26 622 observed 48h post-infection. (B) Bacterial growth measured by qPCR of the 16S rDNA. A lag-phase  
27  
28 623 corresponding to bacterial differentiation of EBs to RBs is observed during the first 5 hours of  
29  
30 624 infection followed by an exponential bacterial growth. An entry into stationary-phase was measured  
31  
32 625 between 16 and 24h post-infection. (C) The replicative cycle was classified in 3 phases: Early, mid  
33  
34 626 and late. The early cycle is characterized by the differentiation of EBs into RBs. Bacterial replication  
35  
36 627 and exponential growth occurs during the mid-phase. The late-phase is characterized by an entry into  
37  
38 628 stationary-phase during which RBs redifferentiate into EBs and by the final cell lysis and release of  
39  
40 629 EBs into the extracellular milieu.  
41  
42

43 630 **Fig 2.** Expression analysis of several housekeeping genes during an infectious cycle to identify the  
44  
45 631 optimal internal control for quantitative reverse transcription analyses (qRT-PCR). (A) Fold increase  
46  
47 632 of 16S rRNA, *gyrB/hsp60-1/secY/rpoB/hc-1* mRNA transcripts and of 16S DNA during a replicative  
48  
49 633 cycle of *Parachlamydia* within *A. castellanii*. DNA extraction was performed with (16S DNA + Lyz +  
50  
51 634 protK) and without proteinase K (16S DNA + Lyz) to obtain DNA extraction method similar to RNA  
52  
53 635 extraction which cannot be performed with proteinase K treatment. Proteinase K treatment is essential  
54  
55 636 to obtain complete lysis of EBs. The fold increase was normalized to 1 at 16h since no difference  
56  
57 637 between samples treated with and without proteinase K is observed at 16h post-infection when the  
58  
59  
60

1  
2  
3 638 bacterial population is only composed of RBs as shown in supplementary figure 1. (B) The ratio  
4  
5 639 between 16S rRNA, *gyrB/hsp60-1/secY/rpoB/hc-1* RNA and 16S DNA was calculated at each time  
6  
7 640 and showed that only 16rRNA is expressed constitutively by exhibiting a ratio 16rRNA/16S DNA of  
8  
9 641 about 1 at each time of the replicative cycle. (C) Temporal transcriptional expression of *gyrB/hsp60-*  
10  
11 642 *1/secY/rpoB/hc-1* normalized to the expression of the internal control 16S rRNA. A significant  
12  
13 643 increase of expression of the essential housekeeping genes *gyrB/hsp60-1/secY/rpoB* is observed  
14  
15 644 during the early to mid-phase of the replicative cycle when EBs differentiate into RBs and during the  
16  
17 645 first-phase of exponential bacterial growth. As previously shown in *C. trachomatis*, the gene encoding  
18  
19 646 for the histone-like protein Hc-1 exhibits an increased expression in the late mid-phase when RBs re-  
20  
21 647 differentiate into EBs.

22  
23  
24 648 **Fig 3.** Temporal transcriptional expression of T3SS genes. (A) Genetic organization of identified  
25  
26 649 T3SS genes (adapted from (Greub *et al.*, 2009)). The identified genes encoding for *Parachlamydia*  
27  
28 650 T3SS proteins are localized in 4 main defined genomic clusters. Clusters 1 to 3 are much conserved  
29  
30 651 among *Chlamydiales* bacteria. A difference is observed for the cluster 4 between *Chlamydiaceae* and  
31  
32 652 other sequenced *Chlamydia*-related bacteria. The conserved genes are represented by different colors  
33  
34 653 according to their respective functions. Hypothetical proteins are represented in light gray and genes  
35  
36 654 encoding for proteins with identified functions likely not involved in T3SS are represented in dark  
37  
38 655 gray. Capital letters refer to set gene names according to the unified nomenclature suggested by Hueck  
39  
40 656 in 1998 (Hueck, 1998). *sycE* and *sycD*: genes encoding for SycE-like and SycD/LcrH-like T3SS  
41  
42 657 chaperones. All SycD/LcrH predicted T3SS chaperones contain conserved tetratricopeptide repeats  
43  
44 658 domains (TPRs). Unlike *Chlamydiaceae*, no genes showing homology with the flagellar system that  
45  
46 659 could have a possible function in chlamydial T3SS have been identified. (B) Transcriptional  
47  
48 660 expression of conserved T3SS genes measured by quantitative reverse transcription PCR (qRT-PCR).  
49  
50 661 The mRNA expression of the various T3SS genes was classified in 4 temporal clusters: EL (early-late  
51  
52 662 phase), L (late-phase), E (early-phase), M (mid-phase) according to the temporal pattern of expression  
53  
54 663 during the replicative cycle. The cluster EL exhibits a marked reduction of mRNA amount during the  
55  
56 664 mid-phase followed by an increased expression in late-phase. Cluster L is characterized by a basal  
57  
58  
59  
60

1  
2  
3 665 expression during early and mid-phase and a significant increased expression during the late-phase.  
4  
5 666 Cluster E is composed of genes that are transcribed during the early and beginning of mid-phase.  
6  
7 667 Finally, the cluster M includes genes that are expressed in the mid-phase.  
8  
9 668

10  
11 669 **Fig 4.** Transcriptional expression cluster analysis of T3SS genes. (A) The highest degree of expression  
12  
13 670 of each gene measured at different time of the infectious cycle was normalized to 100 and the lowest  
14  
15 671 to 0 to generate a matrix of transcriptional expression. The 4 cluster of temporal expression (EL, L, E,  
16  
17 672 M) are indicated on the left part of the matrix. (B) Transcriptional units prediction. A bioinformatic  
18  
19 673 analysis of the T3SS genomic clusters was conducted with the fgenesB software to predict  
20  
21 674 transcriptional units (dotted arrows). Transcriptional units deduced from the experimental  
22  
23 675 transcriptional expression analysis by qRT-PCR (solid arrows). Each gene associated with a predicted  
24  
25 676 transcriptional unit belongs to the same temporal expression cluster. Operon prediction of *C.*  
26  
27 677 *trachomatis* genomic loci containing T3SS genes as described by Hefty and al. (Hefty and Stephens,  
28  
29 678 2007) (dashed arrows). The transcriptional units predicted by the temporal transcriptional clustering of  
30  
31 679 *Parachlamydia* are in congruence with the transcriptional unit prediction of the fgenesB software  
32  
33 680 analysis and/ are highly similar to the operon prediction described in *C. trachomatis*.  
34  
35 681

36  
37 682 **Fig. 5.** Protein expression analysis by western blot. The amount of the T3SS proteins Mscs, SctJ,  
38  
39 683 SctW (CopN), CopB and SycD were analyzed at different times post-infection by western blot using  
40  
41 684 specific mouse antisera. A polyclonal mouse antisera directed against whole bacterial cells was used as  
42  
43 685 an internal control to estimate bacterial number at each time collected during the infectious cycle. The  
44  
45 686 expression of SycD and Mscs was not or poorly detected at 8h and 16h hindering the possibility to  
46  
47 687 measure their relative protein expression during the infectious cycle by western blot. The relative  
48  
49 688 expression of each protein throughout the replicative cycle is roughly estimated at each time by  
50  
51 689 calculating the ratio between the intensity of a given band and the intensity corresponding to whole  
52  
53 690 bacterial number as shown in supplementary Figure 2. Thus, the expression of the protein CopB is  
54  
55 691 induced in the late-phase of the replicative cycle. SctW (CopN) exhibits a significant increased level  
56  
57 692 36h post-infection corresponding to a late-phase expression but the protein is also present in high  
58  
59  
60

1  
2  
3 693 concentrations at 8h post-infection. A high level of SctJ is detected at 8h post-infection corresponding  
4  
5 694 to the early/mid-phase of the replicative cycle.  
6  
7 695

8  
9 696 **Fig. 6.** Quantitative immunofluorescence microscopy. Proteins are labeled by immunofluorescence  
10  
11 697 staining with specific mouse polyclonal antibodies. A series of images of multiple focal planes  
12  
13 698 covering the entire thickness of the sample were collected by z-stack confocal microscopy. Using the  
14  
15 699 ImageJ software, a Z-projection composed of the summing of the slices is generated. The region of  
16  
17 700 interest (ROI) including only the signal of intensity emitted by the bacteria is defined. A histogram of  
18  
19 701 the ROI composed of the signal intensity on the x-axis and of the frequency on the y-axis is generated.  
20  
21 702 A mean value and a standard deviation of the histogram of the frequency distribution of fluorescence  
22  
23 703 intensity are also generated. This method allows the accurate measurement of protein expression at the  
24  
25 704 single cell level.  
26

27 705  
28  
29 706 **Fig. 7.** Protein expression analysis of the late-phase transcribed gene *copB*. CopB was detected with a  
30  
31 707 specific mouse antisera by immunofluorescence staining. (A) Z-projection images generated at  
32  
33 708 different time during infection. Each image contains magnification of various level of CopB  
34  
35 709 expression observed in different bacteria. At 2h post-infection, a heterogenous CopB expression is  
36  
37 710 observed among EBs. Most bacteria exhibit a low CopB expression with only a minor subset showing  
38  
39 711 moderate to high protein expression. CopB expression remains low at 8h post-infection with some  
40  
41 712 RBs expressing CopB moderately. At 16h post-infection, the majority of bacteria poorly expressed  
42  
43 713 CopB but patches of bacteria likely located in the same inclusion exhibit significant increased level of  
44  
45 714 expression. At 24h, 36h and 48h post-infection, most bacteria highly expressed CopB. (B) Histograms  
46  
47 715 of the frequency distribution of fluorescence intensity were generated with each Z-projection showed  
48  
49 716 in panel A. The mean frequency for each histogram was also calculated. These data demonstrate that  
50  
51 717 bacteria induced CopB expression at about 24h post-infection, which corresponds to the  
52  
53 718 transcriptional temporal expression of the *copB* gene (figure 3B).  
54

55  
56 719  
57  
58  
59  
60

1  
2  
3 720 **Fig 8.** Protein expression analysis of Mcsc, SctJ, PahN and SctW (CopN). Two protein (Mcsc and  
4 SctJ) encoded by genes that are transcribed during the early and mid-phase, one protein (PahN)  
5 721 encoded by a mid-phase transcribed gene and one protein (SctW) encoded by a late-phase transcribed  
6 722 gene were analyzed by quantitative immunofluorescence. Similar to transcriptional expression, the  
7 723 Mcsc and SctJ protein exhibit an early to mid-phase increased protein expression at 2h and 8h post-  
8 724 infection followed by a reduced expression during the mid to late-phase of the infection cycle. The  
9 725 expression of the PahN protein was induced during mid-phase and remained highly expressed  
10 726 throughout the rest of the infectious cycle. Relative high amount of SctW were measured 2h post-  
11 727 infection followed by a gradual decrease in protein levels until 16h post-infection. A significant  
12 728 increase in protein expression is then observed in the late-phase cycle at about 24h post-infection,  
13 729 which corresponds to transcriptional expression of the *sctW* gene.  
14 730  
15 731

16  
17  
18  
19  
20  
21  
22  
23  
24  
25  
26  
27 732 **Fig 9.** Model of expression of T3SS components during an infectious cycle of *Parachlamydia* within  
28 733 *A. castellanii*. (A) Schematic overview of the transcriptional expression of the T3SS genes during the  
29 734 3 phases of the replicative cycle. Early-phase: An increased transcriptional expression of  
30 735 *sctC/D/J/T/S/R/L* genes is observed during the early-phase of the cycle. A basal transcriptional  
31 736 expression is observed for the genes encoding other components of the T3SS. Mid-phase: A reduced  
32 737 and moderate expression of *sctC/D/J/T/S/R/L* genes is detected while no change in basal expression of  
33 738 *sctV/N/Q/F/W* genes is observed. The level of *sctU/copB* transcripts is almost undetected suggesting  
34 739 than the transcriptional expression of these genes is highly reduced during the mid-phase of the cycle.  
35 740 In the contrary, the transcriptional expression of the gene encoding for the putative effector protein  
36 741 Pkn5 is significantly induced. Late-phase: A basal expression of the genes *sctC/D/J/T/S/R/L* that were  
37 742 highly expressed during the early-phase is observed whereas an increased transcriptional expression of  
38 743 the genes *sctV/N/Q/F/W/U* and *copB* (or *CopB2*) is measured during the late-phase of replication. (B)  
39 744 Relative T3SS proteins content during the 3 different phases of the cycle. The T3SS is a multi-  
40 745 component complex machinery containing protein with diverse functions and in varying quantities. A  
41 746 varying stoichiometric composition of the T3SS could likely define the functionality of the apparatus.  
42 747 The levels of proteins in bacterial cells are controlled by multiple mechanisms and are defined by both  
43  
44  
45  
46  
47  
48  
49  
50  
51  
52  
53  
54  
55  
56  
57  
58  
59  
60

1  
2  
3 748 the rate of protein synthesis and protein degradation, which are varying with the physiological status  
4  
5 749 of the bacteria during a growth cycle. The relative protein content of the T3SS in EBs is likely similar  
6  
7 750 to the protein content observed during the late-phase of the replicative cycle when RBs redifferentiate  
8  
9 751 into EBs before cell lysis and bacterial release in the extracellular milieu. During that time, the T3SS  
10  
11 752 is likely not required for secretion of bacterial effectors and is maintained in a dormant state ready to  
12  
13 753 be activated. Upon cell contact and bacterial internalization of EBs, the T3SS is likely quickly  
14  
15 754 activated to allow rapid secretion of effector proteins to modulate host cell functions. Rapid de novo  
16  
17 755 synthesis of some T3SS components likely occurs during the critical early-phase of bacterial infection  
18  
19 756 to promote bacterial survival, differentiation, maturation and initiation of replication. The subversion  
20  
21 757 of host cell defense mechanisms has likely to be operated during the early-phase of the infection to  
22  
23 758 ensure bacterial evasion from the lytic pathway. In mid-phase, once the bacteria have established  
24  
25 759 conditions allowing efficient bacterial replication such as replicative vacuole maturation, subversion of  
26  
27 760 host cell defenses and establishment of systems allowing efficient scavenging of host cell nutrients,  
28  
29 761 the importance and the number of T3SS per bacteria are reduced. Finally, increased de novo synthesis  
30  
31 762 of some T3SS components in the late-phase trigger the shutdown of the apparatus (SctW) and the  
32  
33 763 formation of a silent T3SS in EBs ready to be rapidly activated when requested. IM: Inner membrane.  
34  
35 764 OM: Outer membrane. RVM: Replication vacuole membrane  
36  
37

38 765 **Supplementary figure 1.** Proteinase K treatment is required for complete EBs lysis during DNA  
39  
40 766 extraction. Bacterial growth quantified by DNA copy number in a logarithmic (A) and linear (B) scale  
41  
42 767 measured by qPCR during a replicative cycle of *Parachlamydia* within *A. castellanii* from DNA  
43  
44 768 extracted with and without proteinase K treatment. A significant difference is observed when extracted  
45  
46 769 samples contain a bacterial population composed of a majority of EBs demonstrating the absolute  
47  
48 770 requirement of proteinase K treatment for complete bacterial lysis of both EBs and RBs.  
49  
50

51 771 **Supplementary figure 2.** Estimation of protein expression during a replicative cycle by western blot.  
52  
53 772 Total bacterial number was detected with an antisera directed against whole bacterial cells ( $\alpha$ -Para).  
54  
55 773 The relative expression of CopB, SctW (CopN) and SctJ at different times of bacterial growth was  
56  
57 774 estimated by calculating the ratio between the intensity of the bands corresponding to the different  
58  
59  
60

1  
2  
3  
4  
5  
6  
7  
8  
9  
10  
11  
12  
13  
14  
15  
16  
17  
18  
19  
20  
21  
22  
23  
24  
25  
26  
27  
28  
29  
30  
31  
32  
33  
34  
35  
36  
37  
38  
39  
40  
41  
42  
43  
44  
45  
46  
47  
48  
49  
50  
51  
52  
53  
54  
55  
56  
57  
58  
59  
60

775 proteins and the intensity of the signal obtained with total anti-*Parachlamydia* antisera. The results  
776 were normalized to 1 at 8h post-infection.  
777

1  
2  
3 778 **Acknowledgments**  
4

5 779 This work was supported by a grant from the Swiss National Science Foundation no 310030-124843  
6

7 780 & n°310030-141050. We thank Sebastien Aeby for technical assistance. We also thank the Cellular  
8

9 781 Imaging Facility (CIF) of the University of Lausanne for confocal microscopy.  
10

11  
12 782  
13  
14  
15  
16  
17  
18  
19  
20  
21  
22  
23  
24  
25  
26  
27  
28  
29  
30  
31  
32  
33  
34  
35  
36  
37  
38  
39  
40  
41  
42  
43  
44  
45  
46  
47  
48  
49  
50  
51  
52  
53  
54  
55  
56  
57  
58  
59  
60

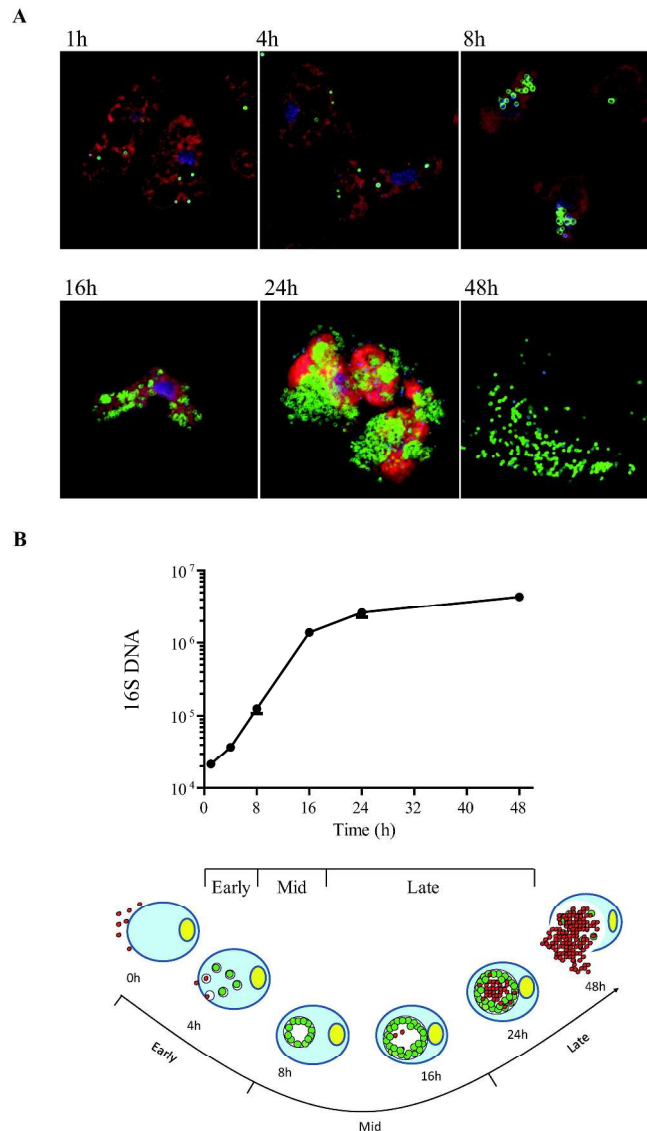


Fig. 1

Fig 1. Temporal characterization of the replicative cycle. (A) *Acanthamoeba castellanii* were infected with *Parachalmydia acanthamoebae* at a MOI of 10 to obtain an amoebal infectious rate of nearly 100% ensuring that only a single infectious cycle occurred in every experiment. Samples were collected at the indicated times post-infection to cover the complete replicative cycle. Bacteria (green) were labeled by immunofluorescence using specific mouse anti-*P. acanthamoebae* polyclonal antibodies. *A. castellanii* (red) were stained with concanavalin A. An average of 2-5 infectious particles per amoebal cell were observed 1h post-infection. Internalization and differentiation of EBs into RBs occurred during the 5 first hours of the infection. Replicating RBs located in bacterial inclusions were observed from 8 to 24h post-infection. Redifferentiation of RBs into EBs occurred between 24-48h post-infection. Finally cell lysis and extrusion of infectious EBs from host cells were observed 48h post-infection. (B) Bacterial growth measured by qPCR of the 16S rDNA. A lag-phase corresponding to bacterial differentiation of EBs to RBs is observed during the first 5 hours of infection followed by an exponential bacterial growth. An entry into stationary-phase was measured between 16 and 24h post-infection. (C) The replicative cycle was classified in 3 phases: Early, mid

1  
2  
3 and late. The early cycle is characterized by the differentiation of EBs into RBs. Bacterial replication and  
4 exponential growth occurs during the mid-phase. The late-phase is characterized by an entry into  
5 stationary-phase during which RBs redifferentiate into EBs and by the final cell lysis and release of EBs into  
6 the extracellular milieu.  
7 262x487mm (300 x 300 DPI)  
8  
9  
10  
11  
12  
13  
14  
15  
16  
17  
18  
19  
20  
21  
22  
23  
24  
25  
26  
27  
28  
29  
30  
31  
32  
33  
34  
35  
36  
37  
38  
39  
40  
41  
42  
43  
44  
45  
46  
47  
48  
49  
50  
51  
52  
53  
54  
55  
56  
57  
58  
59  
60

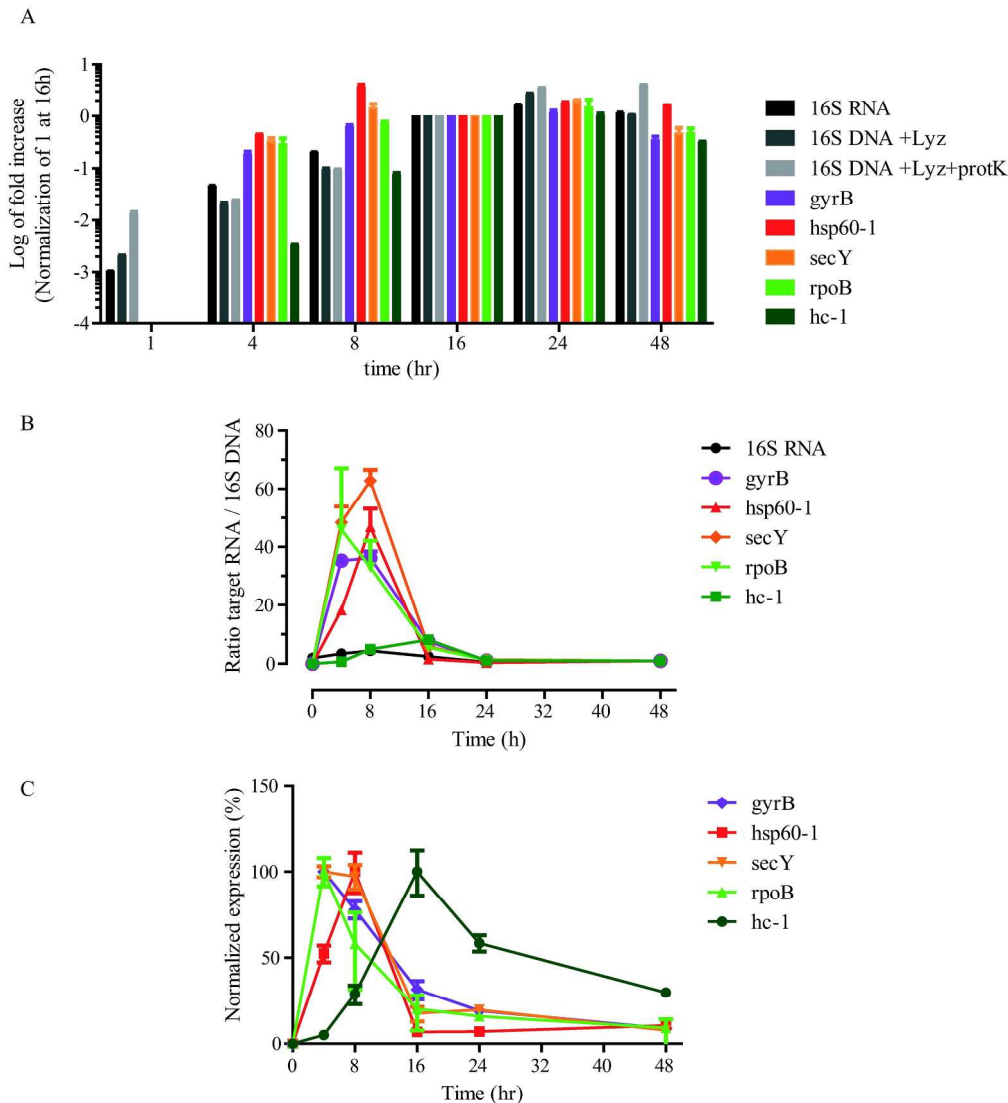


Fig. 2

Fig 2. Expression analysis of several housekeeping genes during an infectious cycle to identify the optimal internal control for quantitative reverse transcription analyses (qRT-PCR). (A) Fold increase of 16S rRNA, gyrB/ hsp60-1/secY/rpoB/ hc-1 mRNA transcripts and of 16S DNA during a replicative cycle of *Parachlamydia* within *A. castellanii*. DNA extraction was performed with (16S DNA + Lyz + protK) and without proteinase K (16S DNA + Lyz) to obtain DNA extraction method similar to RNA extraction which cannot be performed with proteinase K treatment. Proteinase K treatment is essential to obtain complete lysis of EBs. The fold increase was normalized to 1 at 16h since no difference between samples treated with and without proteinase K is observed at 16h post-infection when the bacterial population is only composed of RBs as shown in supplementary figure 1. (B) The ratio between 16S rRNA, gyrB/ hsp60-1/secY/rpoB/ hc-1 RNA and 16S DNA was calculated at each time and showed that only 16rRNA is expressed constitutively by exhibiting a ratio 16rRNA/16S DNA of about 1 at each time of the replicative cycle. (C) Temporal transcriptional expression of gyrB/ hsp60-1/secY/rpoB/ hc-1 normalized to the expression of the internal control 16S rRNA. A significant increase of expression of the essential housekeeping genes gyrB/ hsp60-1/secY/rpoB is observed during the early to mid-phase of the replicative cycle when EBs differentiate into

1  
2  
3 RBs and during the first-phase of exponential bacterial growth. As previously shown in *C. trachomatis*, the  
4 gene encoding for the histone-like protein Hc-1 exhibits an increased expression in the late mid-phase when  
5 RBs re-differentiate into EBs.  
6  
7  
8  
9  
10  
11  
12  
13  
14  
15  
16  
17  
18  
19  
20  
21  
22  
23  
24  
25  
26  
27  
28  
29  
30  
31  
32  
33  
34  
35  
36  
37  
38  
39  
40  
41  
42  
43  
44  
45  
46  
47  
48  
49  
50  
51  
52  
53  
54  
55  
56  
57  
58  
59  
60

233x277mm (300 x 300 DPI)

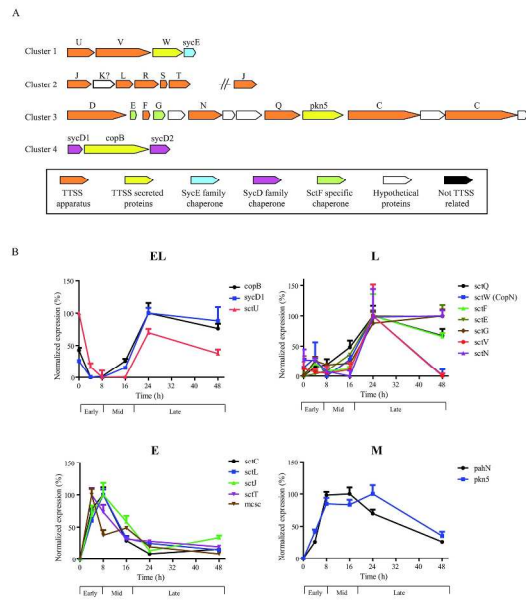


Fig. 3

Fig 3. Temporal transcriptional expression of T3SS genes. (A) Genetic organization of identified T3SS genes (adapted from (Greub et al., 2009)). The identified genes encoding for *Parachlamydia* T3SS proteins are localized in 4 main defined genomic clusters. Clusters 1 to 3 are much conserved among *Chlamydiales* bacteria. A difference is observed for the cluster 4 between *Chlamydiaceae* and other sequenced *Chlamydia*-related bacteria. The conserved genes are represented by different colors according to their respective functions. Hypothetical proteins are represented in light gray and genes encoding for proteins with identified functions likely not involved in T3SS are represented in dark gray. Capital letters refer to sct gene names according to the unified nomenclature suggested by Hueck in 1998 (Hueck, 1998). *sycE* and *sycD*: genes encoding for SycE-like and SycD/LcrH-like T3SS chaperones. All SycD/LcrH predicted T3SS chaperones contain conserved tetratricopeptide repeats domains (TPRs). Unlike *Chlamydiaceae*, no genes showing homology with the flagellar system that could have a possible function in chlamydial T3SS have been identified. (B) Transcriptional expression of conserved T3SS genes measured by quantitative reverse transcription PCR (qRT-PCR). The mRNA expression of the various T3SS genes was classified in 4 temporal clusters: EL (early-late phase), L (late-phase), E (early-phase), M (mid-phase) according to the temporal pattern of expression during the replicative cycle. The cluster EL exhibits a marked reduction of mRNA amount during the mid-phase followed by an increased expression in late-phase. Cluster L is characterized by a basal expression during early and mid-phase and a significant increased expression during the late-phase. Cluster E is composed of genes that are transcribed during the early and beginning of mid-phase. Finally, the cluster M includes genes that are expressed in the mid-phase.

263x174mm (300 x 300 DPI)

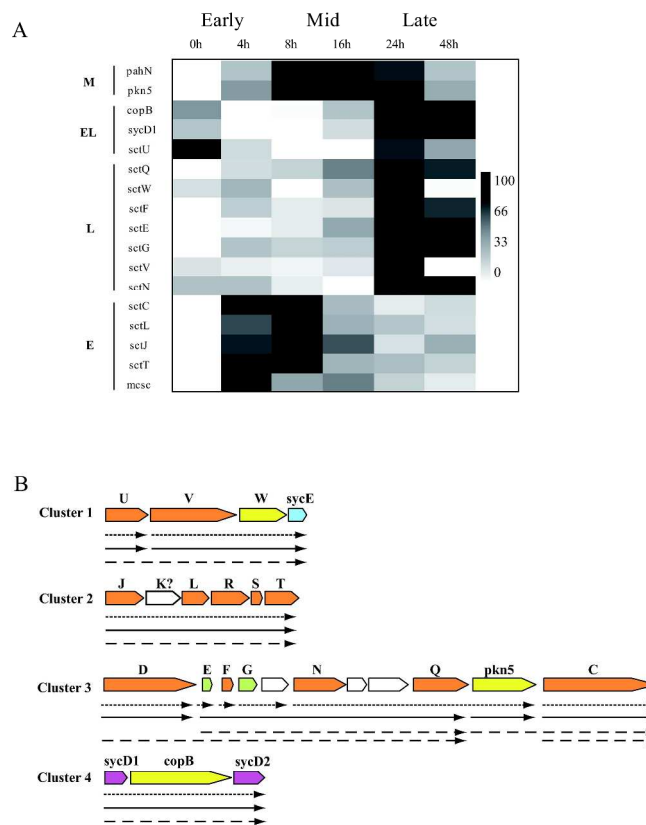


Fig. 4

Fig 4. Transcriptional expression cluster analysis of T3SS genes. (A) The highest degree of expression of each gene measured at different time of the infectious cycle was normalized to 100 and the lowest to 0 to generate a matrix of transcriptional expression. The 4 cluster of temporal expression (EL, L, E, M) are indicated on the left part of the matrix. (B) Transcriptional units prediction. A bioinformatic analysis of the T3SS genomic clusters was conducted with the fgenesB software to predict transcriptional units (dotted arrows). Transcriptional units deduced from the experimental transcriptional expression analysis by qRT-PCR (solid arrows). Each gene associated with a predicted transcriptional unit belongs to the same temporal expression cluster. Operon prediction of *C. trachomatis* genomic loci containing T3SS genes as described by Hefty and al. (Hefty and Stephens, 2007) (dashed arrows). The transcriptional units predicted by the temporal transcriptional clustering of *Parachlamydia* are in congruence with the transcriptional unit prediction of the fgenesB software analysis and/ are highly similar to the operon prediction described in *C. trachomatis*.

304x444mm (300 x 300 DPI)

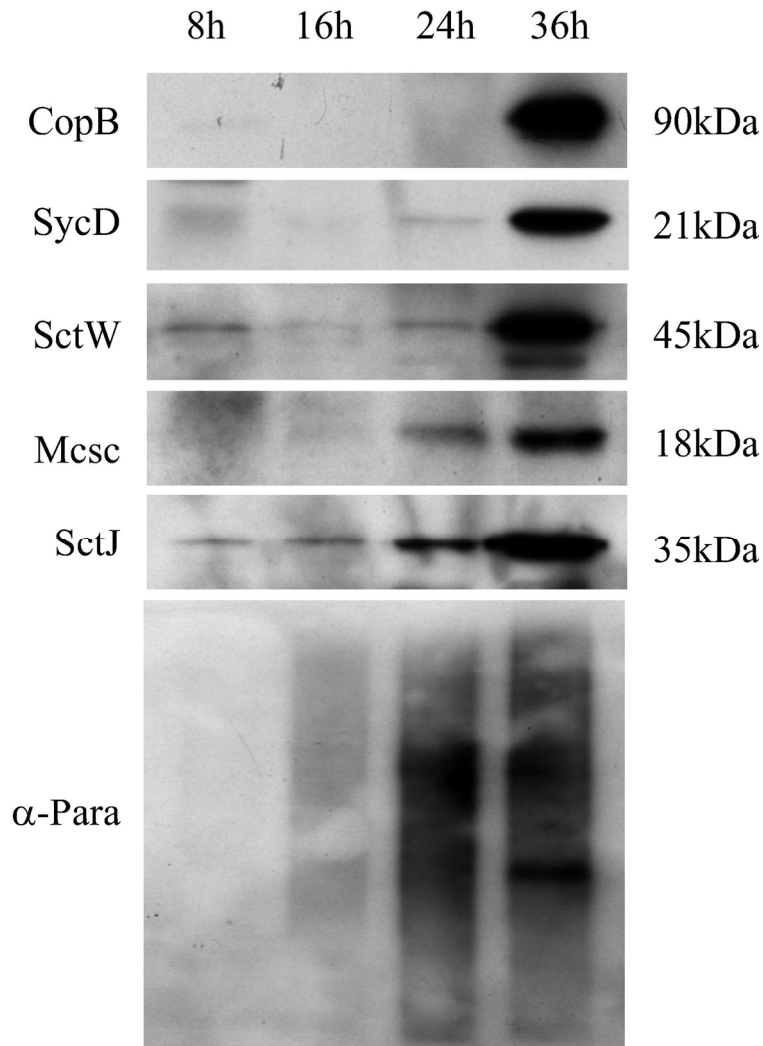
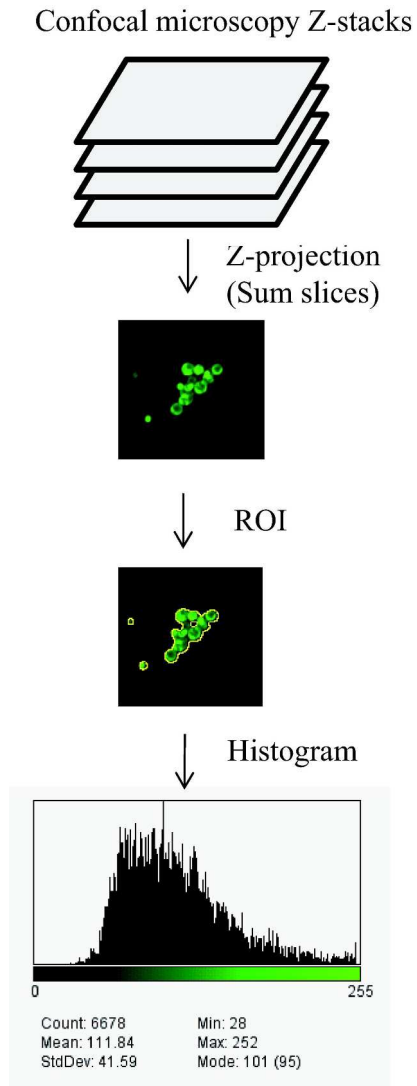


Fig.5

Fig. 5. Protein expression analysis by western blot. The amount of the T3SS proteins Mcsc, SctJ, SctW (CopN), CopB and SycD were analyzed at different times post-infection by western blot using specific mouse antisera. A polyclonal mouse antisera directed against whole bacterial cells was used as an internal control to estimate bacterial number at each time collected during the infectious cycle. The expression of SycD and Mcsc was not or poorly detected at 8h and 16h hindering the possibility to measure their relative protein expression during the infectious cycle by western blot. The relative expression of each protein throughout the replicative cycle is roughly estimated at each time by calculating the ratio between the intensity of a given band and the intensity corresponding to whole bacterial number as shown in supplementary Figure 2. Thus, the expression of the protein CopB is induced in the late-phase of the replicative cycle. SctW (CopN) exhibits a significant increased level 36h post-infection corresponding to a late-phase expression but the protein is also present in high concentrations at 8h post-infection. A high level of SctJ is detected at 8h post-infection corresponding to the early/mid-phase of the replicative cycle.

127x204mm (300 x 300 DPI)



46  
47  
48  
49  
50  
51  
52  
53  
54  
55  
56  
57  
58  
59  
60

Fig. 6

Fig. 6. Quantitative immunofluorescence microscopy. Proteins are labeled by immunofluorescence staining with specific mouse polyclonal antibodies. A series of images of multiple focal planes covering the entire thickness of the sample were collected by z-stack confocal microscopy. Using the ImageJ software, a Z-projection composed of the summing of the slices is generated. The region of interest (ROI) including only the signal of intensity emitted by the bacteria is defined. A histogram of the ROI composed of the signal intensity on the x-axis and of the frequency distribution of fluorescence intensity are also generated. This method allows the accurate measurement of protein expression at the single cell level.

164x491mm (300 x 300 DPI)

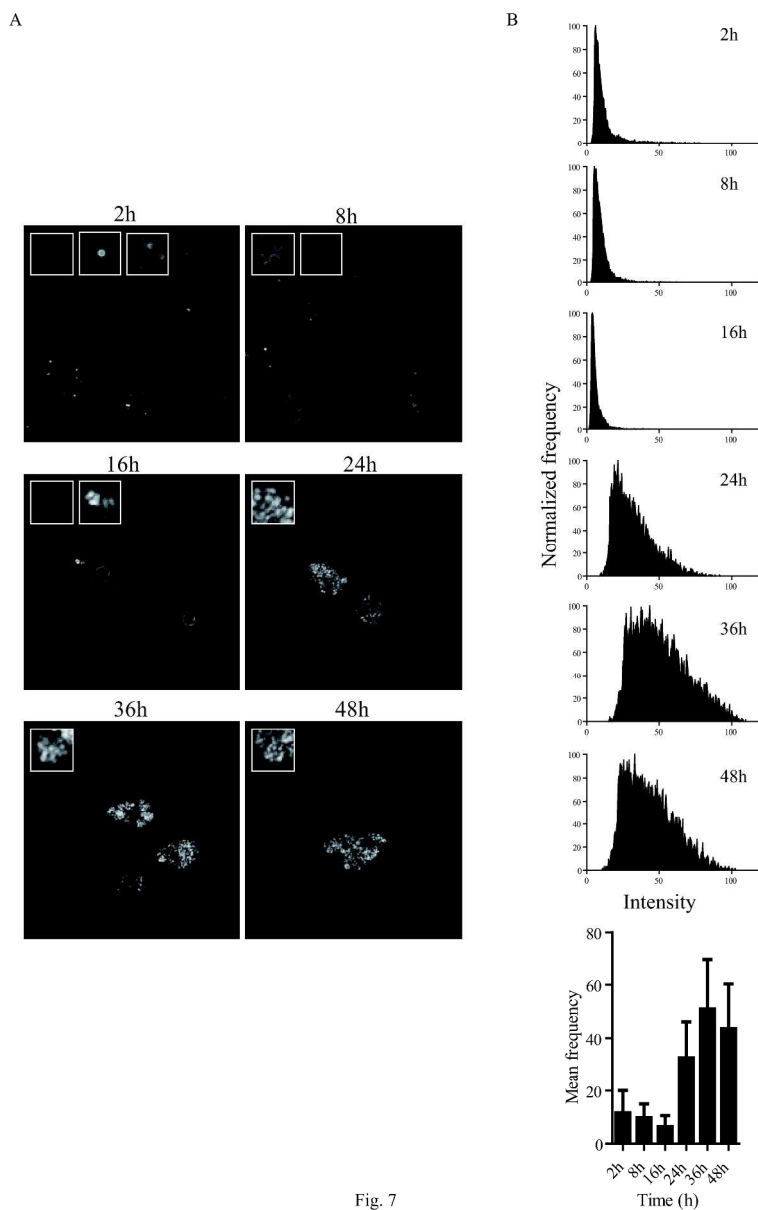


Fig. 7

Fig. 7. Protein expression analysis of the late-phase transcribed gene *copB*. *CopB* was detected with a specific mouse antisera by immunofluorescence staining. (A) Z-projection images generated at different time during infection. Each image contains magnification of various level of *CopB* expression observed in different bacteria. At 2h post-infection, a heterogenous *CopB* expression is observed among EBs. Most bacteria exhibit a low *CopB* expression with only a minor subset showing moderate to high protein expression. *CopB* expression remains low at 8h post-infection with some RBs expressing *CopB* moderately. At 16h post-infection, the majority of bacteria poorly expressed *CopB* but patches of bacteria likely located in the same inclusion exhibit significant increased level of expression. At 24h, 36h and 48h post-infection, most bacteria highly expressed *CopB*. (B) Histograms of the frequency distribution of fluorescence intensity were generated with each Z-projection showed in panel A. The mean frequency for each histogram was also calculated. These data demonstrate that bacteria induced *CopB* expression at about 24h post-infection, which corresponds to the transcriptional temporal expression of the *copB* gene (figure 3B).

283x451mm (300 x 300 DPI)

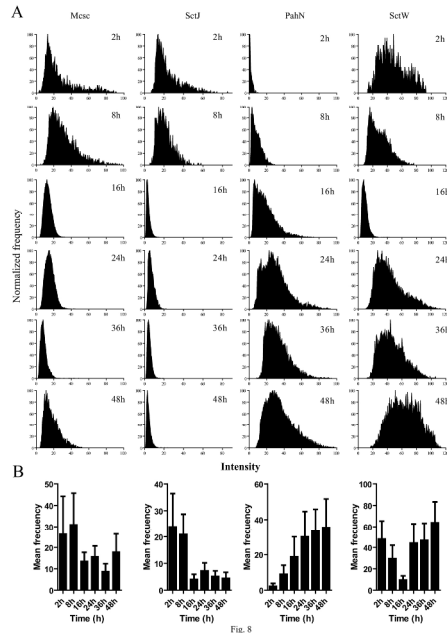


Fig. 8

Fig 8. Protein expression analysis of Mcsc, SctJ, PahN and SctW (CopN). Two protein (Mcsc and SctJ) encoded by genes that are transcribed during the early and mid-phase, one protein (PahN) encoded by a mid-phase transcribed gene and one protein (SctW) encoded by a late-phase transcribed gene were analyzed by quantitative immunofluorescence. Similar to transcriptional expression, the Mcsc and SctJ protein exhibit an early to mid-phase increased protein expression at 2h and 8h post-infection followed by a reduced expression during the mid to late-phase of the infectious cycle. The expression of the PahN protein was induced during mid-phase and remained highly expressed throughout the rest of the infectious cycle. Relative high amount of SctW were measured 2h post-infection followed by a gradual decrease in protein levels until 16h post-infection. A significant increase in protein expression is then observed in the late-phase cycle at about 24h post-infection, which corresponds to transcriptional expression of the sctW gene.

297x187mm (300 x 300 DPI)

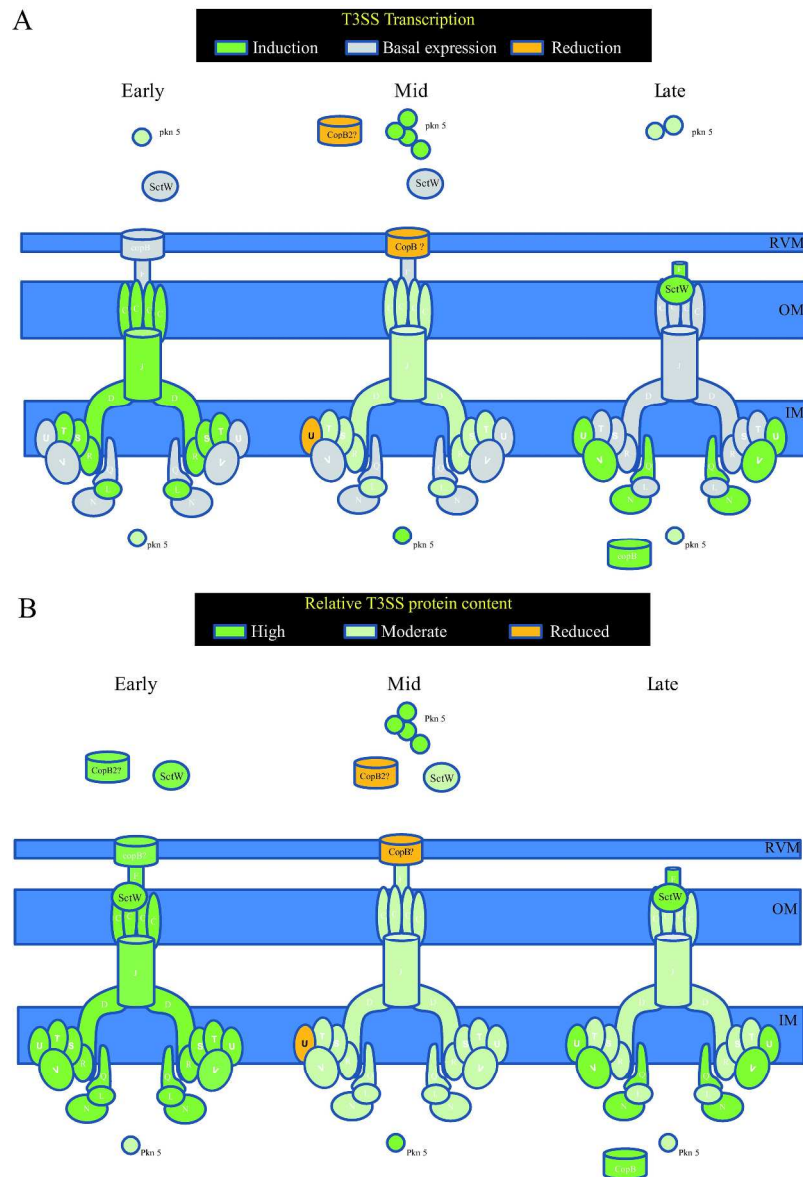


Fig. 9

Fig 9. Model of expression of T3SS components during an infectious cycle of *Parachlamydia* within *A. castellanii*. (A) Schematic overview of the transcriptional expression of the T3SS genes during the 3 phases of the replicative cycle. Early-phase: An increased transcriptional expression of *sctC/D/J/T/S/R/L* genes is observed during the early-phase of the cycle. A basal transcriptional expression is observed for the genes encoding other components of the T3SS. Mid-phase: A reduced and moderate expression of *sctV/N/Q/F/W* genes is observed while no change in basal expression of *sctC/D/J/T/S/R/L* genes is detected. The level of *sctU/copB* transcripts is almost undetected suggesting that the transcriptional expression of these genes is highly reduced during the mid-phase of the cycle. In the contrary, the transcriptional expression of the gene encoding for the putative effector protein Pkn5 is significantly induced. Late-phase: A basal expression of the genes *sctC/D/J/T/S/R/L* that were highly expressed during the early-phase is observed whereas an increased transcriptional expression of the genes *sctV/N/Q/F/W/U* and *copB* (or CopB2) is measured during the late-phase of replication. (B) Relative T3SS proteins content during the 3 different phases of the cycle. The T3SS is a multi-component complex machinery containing protein with

1  
2  
3 diverse functions and in varying quantities. A varying stoichiometric composition of the T3SS could likely  
4 define the functionality of the apparatus. The levels of proteins in bacterial cells are controlled by multiple  
5 mechanisms and are defined by both the rate of protein synthesis and protein degradation, which are  
6 varying with the physiological status of the bacteria during a growth cycle. The relative protein content of  
7 the T3SS in EBs is likely similar to the protein content observed during the late-phase of the replicative cycle  
8 when RBs redifferentiate into EBs before cell lysis and bacterial release in the extracellular milieu. During  
9 that time, the T3SS is likely not required for secretion of bacterial effectors and is maintained in a dormant  
10 state ready to be activated. Upon cell contact and bacterial internalization of EBs, the T3SS is likely quickly  
11 activated to allow rapid secretion of effector proteins to modulate host cell functions. Rapid de novo  
12 synthesis of some T3SS components likely occurs during the critical early-phase of bacterial infection to  
13 promote bacterial survival, differentiation, maturation and initiation of replication. The subversion of host  
14 cell defense mechanisms has likely to be operated during the early-phase of the infection to ensure bacterial  
15 evasion from the lytic pathway. In mid-phase, once the bacteria have established conditions allowing  
16 efficient bacterial replication such as replicative vacuole maturation, subversion of host cell defenses and  
17 establishment of systems allowing efficient scavenging of host cell nutrients, the importance and the number  
18 of T3SS per bacteria are reduced.  
19  
20  
21  
22  
23  
24  
25  
26  
27  
28  
29  
30  
31  
32  
33  
34  
35  
36  
37  
38  
39  
40  
41  
42  
43  
44  
45  
46  
47  
48  
49  
50  
51  
52  
53  
54  
55  
56  
57  
58  
59  
60